Synergistic control of chloroplast biogenesis by *MYB-related* and *Golden2-like* transcription factors

Eftychios Frangedakis[1,*,$], Nataliya E. Yelina[1,2,*], Kumari Billakurthi[1], Tina Schreier[1,3], Patrick J. Dickinson[1], Marta Tomaselli[1], Jim Haseloff[1], Julian M. Hibberd[1,$]

[1]Department of Plant Sciences, University of Cambridge, Cambridge, CB3 EA, UK

[2]Present address: Crop Science Centre, University of Cambridge, 93 Lawrence Weaver Road, Cambridge CB3 0LE, UK

[3]Present address: Department of Biology, University of Oxford, South Parks Road, Oxford OX1 3RB, UK

* equal contribution

$ correspondence:

Julian M. Hibberd

jmh65@cam.ac.uk

Eftychios Frangedakis

ef391@cam.ac.uk

Keywords: *Chloroplast biogenesis, photosynthesis, Marchantia, Arabidopsis, transcription factors*

Abstract

Chloroplast biogenesis is dependent on master regulators from the GOLDEN2-LIKE (GLK) family of transcription factors, but *glk* mutants contain residual chlorophyll and therefore other proteins must also be involved. Here we identify MYB-related transcription factors as regulators of chloroplast biogenesis in the liverwort *Marchantia polymorpha* and angiosperm *Arabidopsis thaliana*. In both species, double mutant alleles in MYB-Related genes show very limited chloroplast development, and photosynthesis gene expression is perturbed to a greater extent than in mutants of *GLK*. In *M. polymorpha* MYB-related genes act upstream of *GLK*, while in *A. thaliana* this relationship has been rewired. In both species, genes encoding enzymes of chlorophyll biosynthesis are controlled by MYB-related and GLK proteins whilst those allowing CO_2 fixation, photorespiration and photosystem assembly and repair require the MYB-related proteins. Thus, *MYB-related* and *GLK* genes have overlapping as well as distinct targets. We conclude that together MYB-related and GLK transcription factors orchestrate chloroplast development in land plants.

Introduction

Photosynthesis is fundamental to life and in eukaryotes takes place in organelles known as chloroplasts. It is widely accepted that chloroplasts originated from endosymbiosis between a photosynthetic prokaryote and heterotrophic eukaryote that was initiated more than one billion years ago.[1–3] Since then, significant elaborations to the control of photosynthesis gene expression have taken place. For example, in plants the majority of genes allowing chloroplast biogenesis are encoded in the nucleus such that thousands are post-translationally imported from cytosol to chloroplast.[4,5] Despite these significant rearrangements to the genetics of photosynthesis in most plants including major crops, the photosynthetic process has not been optimised by natural selection.[6,7] One current limitation to improving photosynthesis in crops is knowledge of the underlying gene regulatory networks.

The expression of photosynthesis associated nuclear genes is responsive to light and also to processes intrinsic to the cell. For example, in angiosperms light is required for chloroplast formation, but hormones amplify or repress this response.[8] These exogenous and endogenous inputs are integrated by key transcriptional regulators belonging to the GOLDEN2-LIKE (GLK) and GATA families of transcription factors (GATA Nitrate-inducible Carbon metabolism-involved [GNC] and Cytokinin-Responsive GATA Factor 1 [CGA1].[8–12] However, *glk* mutants in *Arabidopsis thaliana*[10], rice[13] and also non-seed plants such as *Physcomitrium patens*[14] and *Marchantia polymorpha*[15] still contain chlorophyll. Moreover, mutants lacking functional *GLK* and *GATA* genes are not albino.[9,16] In summary, other actors must allow assembly of the photosynthetic apparatus in the absence of these known regulators.

We therefore sought to identify new transcription factors acting alongside the master regulator GLK. As forward genetics has failed to identify such proteins, we rationalised that genetic redundancy had hindered their identification and that analysis of a species with a more compact genome would circumvent this issue. *Marchantia polymorpha* possesses a streamlined genome with many transcription factors represented by either one or two copies and the dominant form of the lifecycle is haploid.[17] Moreover, control of greening is streamlined with only one copy of *GLK* being present, and orthologs of *GATAs* implicated in chloroplast biogenesis in other land plants[18] not being required.[15] We hypothesised that homologous transcription factors in *A. thaliana* and *M. polymorpha* act alongside *GLK* and so their expression should respond to light during photomorphogenesis in both species. After re-examination of publicly available RNA sequencing data, gene editing of transcription factors and detailed phenotypic analysis we identify two RR-MYB transcription factors as regulators of chloroplast biogenesis and photosynthesis gene expression in *M. polymorpha* and *A. thaliana*. In contrast to the GLK proteins that regulate expression of genes allowing chlorophyll biosynthesis and function of photosystem I and II, the RR-MYBs have a broader set of targets that extends to genes allowing CO_2 fixation, photorespiration, photosystem assembly and repair. We conclude that these proteins function as master regulators of chloroplast biogenesis and photosynthesis gene expression. The data have implications for understanding chloroplast

biogenesis and photosynthesis as well as other processes taking place in plastids such as nitrogen and sulphur assimilation, the biosynthesis of amino acids, fatty acids and carotenoids.

Results

Mp*RR-MYB5* regulates chloroplast development synergistically with its paralog Mp*RR-MYB2*

We interrogated publicly available gene expression data sampled during the transition from non-photosynthetic to photosynthetic growth in *M. polymorpha*[19] as well as *A. thaliana.*[20] This identified 108 and 144 transcription factors that were upregulated after exposure to light in *M. polymorpha* and *A. thaliana* respectively **(Table S1 and S2)**. We then selected orthologs upregulated in both datasets with an unknown or chlorophyll-related annotation that were represented by a multigene family in *A. thaliana* **(Figure 1A)**. Fourteen candidates from *M. polymorpha* were identified **(Figure 1B and Table S2)**. Two of these (Mp*GLK,* Mp*GATA4*) are homologs of known photosynthesis regulators in *A. thaliana*[10,21] and Mp*GLK* has a confirmed role in *M. polymorpha.*[15] The remainder included a number of B-BOX (BBX) domain proteins known to interact with the master regulator of photomorphogenesis HY5[22], a homeobox-leucine zipper (HD-ZIP) protein *ATHB17* whose ortholog in *A. thaliana* regulates photosynthesis-associated nuclear genes in response to abiotic stress,[23] a *C2H2* type zinc finger transcription factor with unknown function in *A. thaliana,* and a *MYB-related* gene predicted to regulate photosynthesis gene expression.[24,25]

Taking advantage of the rapid and predominantly haploid life-cycle we used *M. polymorpha* as a testbed for each of these candidates and subjected each to CRISPR/Cas9-mediated editing. With the exception of Mp*GLK*, which has previously been reported to lead to a pale phenotype when mutated[15] only one other candidate had low chlorophyll. This was Mp5g11830, annotated as Mp*RR-MYB5* in the *M. polymorpha* genome database*,* but previously also referred to as a CIRCADIAN CLOCK ASSOCIATED1-like RR-MYB-Related transcription factor.[26,27] Mp*RR-MYB5* has a single paralog (Mp*RR-MYB2* - **Figure 1C**) that shows high similarity to Mp*RR-MYB5* at the amino acid level (**Figure 1C**) with for example the CCA1-like/RR-Myb domain being 92% identical (**Figure 1C**). Mutant alleles of Mp*RR-MYB5* but not Mp*RR-MYB2* appeared pale (**Figure 1D, E, F, Figure S1A-B**) and analysis of chlorophyll content confirmed this (**Figure 1H**). All lines in which insertions or deletions introduced premature stop codons in Mp*RR-MYB5* (**Figure S1A**) had 40-50% less chlorophyll than controls (**Figure 1E and H**). The Mp*rr-myb5* mutant was complemented when Mp*RR-MYB5* was expressed from its own promoter (**Figure S1C**) confirming that the pale phenotype was unlikely associated with off-target CRISPR/Cas9 editing. Mutating Mp*RR-MYB5* and Mp*RR-MYB2* simultaneously (**Figure S1D**) led to extremely pale plants with chlorophyll content reduced to 95% compared with controls (**Figure 1G and H**). To test whether the photosynthetic apparatus was functional in the single Mp*rr-myb5* and double Mp*rr-myb5,2* mutants we applied the inhibitor Di-Chlorophenyl Di-Methyl Urea (DCMU) that blocks photosynthetic electron transport[28] and measured activity of photosystem II via chlorophyll fluorescence imaging. This showed that although these mutants had low levels of chlorophyll, the photosynthetic apparatus was operational (**Figure 1I**). Consistent with the very low chlorophyll levels in Mp*rr-myb5*, and Mp*rr-myb5,2* double mutants, chloroplasts were significantly smaller and thylakoids underdeveloped (**Figure 1J-R and Figure**

S1E). It was noticeable that poorly developed chloroplasts from double Mp*rr-myb5*,*2* mutants contained significant amounts of starch.

To determine whether Mp*RR-MYB5* and Mp*RR-MYB2* limit greening, we generated overexpression lines driven by the strong Mp*UBE2* constitutive promoter[29] and to facilitate analysis of chloroplast size per cell used GFP to mark the plasma membrane (**Figure S2A-E**). Although quantitative polymerase chain reactions confirmed that each transgene was over-expressed (**Figure S2F-N**) plants appeared similar to controls and there were no evident perturbations to chlorophyll content, chloroplast size or morphology (**Figure S2O-P**). We conclude that Mp*RR-MYB5* and Mp*RR-MYB2* act redundantly and are necessary for chloroplast biogenesis but in contrast with Mp*GLK*[15] they are not sufficient to activate this process. Moreover, in the absence of both Mp*RR-MYB5* and Mp*RR-MYB2* assembly of the photosynthetic apparatus is very limited.

Mp*RR-MYB5&2* act with Mp*GLK* to control chloroplast biogenesis

As double Mp*rr-myb5*,*2* mutants showed residual chloroplast development and were viable, we hypothesised that the limited ability for photoautotrophic growth was associated with activity of the previously characterised master regulator *GLK*. To test this, we attempted to generate higher order mutants which combined mutant alleles of Mp*glk*, Mp*rr-myb5* and Mp*rr-myb2*. We were able to knock out Mp*RR-MYB5* in the presence of Mp*glk* mutant alleles (**Figure S3A-B**). Such double mutants were paler than the single Mp*glk* mutant (**Figure 2A-D**) and contained less chlorophyll (**Figure 2E**). Application of DCMU confirmed that the photosystem II was functional in the Mp*glk*,*rr-myb5* double mutant (**Figure 2F**). Double Mp*glk,rr-myb5* mutants had smaller chloroplasts with fewer thylakoid membranes and reduced granal stacking compared with each single mutant (**Figure 2G-O**). Thus, in the absence of both Mp*RR-MYB5* and MpGLK, very limited assembly of the photosynthetic apparatus takes place.

We were unable to generate triple Mp*glk,rr-myb5,2* mutants implying that this allelic combination is lethal. For example, after super transforming Mp*glk,rr-myb5* double mutants with a vector allowing expression of the same guide RNA used to generate the single Mp*rr-myb2* mutants reported above, 91 lines were obtained. However, none were paler than the double Mp*glk,rr-myb5* mutant, and when genotyped 86 lines had no edits in Mp*RR-MYB2*. Of the five lines that were edited in Mp*RR-MYB2* (as well as Mp*GLK* and Mp*RR-MYB5*) genotyping showed that the mutations had limited impact on the MpRR-MYB2 protein. For example, these edits altered one, two, three or seven amino acids in a poorly conserved region of the protein, and in all cases reading frame was maintained (**Figure S3C and D**). In contrast, when the original single Mp*rr-myb2* mutants were identified (**Figure 2F**) 50% of plants contained mutations that introduced early stop codons or disturbed the reading frame. We conclude that absence of all three proteins (MpGLK, MpRR-MYB5 and MpRR-MYB2) is lethal likely because chloroplast biogenesis is abolished.

MpRR-MYB transcription factors regulate genes allowing carbon fixation, photorespiration and photosystem function

To provide insight into the types of genes regulated by Mp*RR-MYB5* and Mp*RR-MYB2* we performed RNA sequencing of overexpressing lines as well as single and multiple mutants. Overexpression of Mp*RR-MYB2* and Mp*RR-MYB5* led to the upregulation of 71 and 11 genes respectively (*padj*-value ≤0.01, LFC ≥ 1-fold) (**Figure S4A and C**) and there was limited overlap between these two datasets (**Figure 3A and Figure S4G and H**). This contrasts with overexpression of Mp*GLK* that led to the upregulation of 492 genes (**Figure 3A** and [15]).

In loss of function mutants for Mp*RR-MYB2* or Mp*RR-MYB5*, 65 and 823 genes, respectively, showed reductions in transcript abundance compared with controls (*padj*-value ≤0.01, LFC ≥ 1-fold) (**Figure 3B and Figure S4B and D**). Knocking out Mp*GLK* had greater impact with 1065 genes being downregulated (**Figure 3B** and [15]). In double Mp*glk,rr-myb5* mutants, 1161 genes had lower transcript abundance than controls, and in the double Mp*rr-myb5,2* mutants this was increased to 1744 (**Figure 3B**). The largest overlap in changes to transcript abundance between genotypes (524 genes) was detected for Mp*glk,rr-myb5* and Mp*rr-myb5,2* mutants (**Figure 3B**). This finding further supports synergistic action of Mp*RR-MYBs* and Mp*GLK*. Gene Ontology (GO) terms were used to provide insight into the classes of genes impacted by overexpression or loss of function of Mp*RR-MYBs* and Mp*GLK*. Consistent with the lack of detectable phenotype after overexpression of Mp*RR-MYB5* or Mp*RRMYB2,* or loss of Mp*RR-MYB2* function, no distinct GO terms were impacted in these lines. Although the response to oxidative stress GO term was over-represented in both Mp*rr-myb5* and Mp*glk* mutants, other terms were distinct (**Figure 3C**). For example, Mp*rr-myb5* mutants showed changes to protein phosphorylation and peroxidase activity terms, whilst in Mp*glk* photosynthesis, light harvesting and chlorophyll biosynthesis terms were affected (**Figure 3C** and [15]). It was notable that very similar GO terms responded in Mp*rr-myb5,2*, Mp*glk* and Mp*glk,rr-myb5* mutants (**Figure 3C**). For example, in all genotypes the top five biological processes impacted were response to oxidative stress, hydrogen peroxide catabolism, photosynthesis, light harvesting and chlorophyll biosynthesis (**Figure 3C**). Thus, loss of function alleles for Mp*rr-myb5,2,* Mp*glk* and Mp*glk,rr-myb5* all caused changes in GO terms primarily associated with photosynthesis.

Since chlorophyll content was reduced in Mp*rr-myb5* and Mp*rr-myb5,2* double mutants we examined impact on transcript abundance derived from genes associated with the nineteen annotated chlorophyll biosynthesis genes (**Figure 3D**). With the exception of the *HEMA* gene in Mp*rr-myb5* mutants*,* knocking out either Mp*RR-MYB5* or Mp*RR-MYB2* did not significantly affect transcript abundance from chlorophyll biosynthesis genes. In contrast, in Mp*glk* mutant alleles transcript abundance from seventeen chlorophyll biosynthesis genes was reduced, and in the Mp*rr-myb5,2* double mutant all nineteen genes were significantly downregulated (**Figure 3D**). We next examined the impact of loss of the Mp*RR-MYBs* on approximately 200 other genes annotated as photosynthesis related in *M. polymorpha* (**Dataset S1**). This group included genes associated with CO_2 fixation and the light harvesting apparatus as well as their assembly and repair. In the single

Mp*rr-myb5* and Mp*rr-myb2* mutant alleles there was limited effect on photosynthesis associated genes (**Figure 3E and Figure 4A**). For example, in Mp*rr-myb2* expression of only a single photosynthesis gene (petE Mp4g02720) was perturbed (**Dataset S2**). In Mp*rr-myb5* mutants, a small number of genes were impacted including those encoding a small subunit of RuBisCO (Mp4g09890) and a CHLOROPHYLL A/B BINDING PROTEIN (Mp7g05530) (**Figure 3E and Dataset S2**). As expected, changes to photosynthesis transcripts were more evident in the Mp*glk* mutant (**Figure 3E and Figure 4A**), and even more severe when both Mp*RR-MYB5* and Mp*GLK* were mutated (**Figure 3E and Figure 4A**). Strikingly, when Mp*RR-MYB2* and Mp*RR-MYB5* were simultaneously knocked out, the effect on photosynthesis associated genes was extensive and more widespread than in the *Mpglk,rr-myb5* double mutant. For example, in Mp*rr-myb5,2* double mutants, the majority of genes encoding enzymes involved in the Calvin Benson Bassham cycle and photorespiration were downregulated (**Figure 3E and Figure S3I**). Moreover, genes encoding components of both photosystems and their respective light harvesting complexes as well as the Cytochrome b_6f complex were downregulated (**Figure 4A**). We also found that genes associated with assembly of RuBisCO, non-photochemical quenching, as well as granal stacking and repair of photosystem II were impacted in Mp*rr-myb5,2* double mutants (**Figure S3J**). This contrasts with Mp*glk* in which only genes encoding enzymes of chlorophyll biosynthesis as well as components of the photosystems and their light harvesting complexes were mis-regulated (**Figure 4A**).

MpRR-MYB transcription factors condition expression of *GLK*

Consistent with the alterations in transcript abundance described above, consensus binding sites for the GLK and RR-MYBs proteins derived from ChIP-seq data[25] and DAP-seq[30] were found in promoters of 37% of photosynthesis genes (**Figure 4B**). 18% and 16% possessed motifs associated with GLK and RR-MYB binding respectively, and 3% contained both motifs (**Figure 4C and Dataset S3**). To test whether GLK and RR-MYB binding sites were enriched in photosynthesis genes above that expected by chance, we determined the frequency of these motifs in 500 base pairs upstream of 159 *M. polymorpha* photosynthesis genes compared with 1000 random sets of 159 *M. polymorpha* promoters (**Figure 4D**). 500bp was selected in order to focus analysis on core promoters rather than long distance enhancer elements and to reduce background signal associated with the increased probability of finding any motif by chance as the search space is greater (**Table S1**). Far fewer photosynthesis genes contained neither motif than would be expected from the background (p-value=0.002) whilst RR-MYB motifs were strongly enriched in photosynthesis genes (p-value=0.002). GLK motifs were over-represented compared with most background sets (p-value=0.078) although this enrichment was weaker than that for RR-MYB motifs. Overall, these data are consistent with overlapping as well as distinct roles for the two classes of transcription factor. Our data also support the notion that in contrast with Mp*GLK*, the Mp*RR-MYBs* activate genes allowing CO_2 fixation as well as light harvesting.

To better understand this interplay between Mp*RR-MYB2,* Mp*RR-MYB5* and Mp*GLK* we first examined the expression of Mp*RR-MYB2&5* in the *Mpglk* mutant background. Mp*RR-MYB5* and Mp*RR-MYB2* were upregulated in Mp*glk* (**Figure 4E**), a finding consistent with Mp*GLK* acting to repress Mp*RR-MYB5&2*. In contrast, in the Mp*rr-myb5,2* double mutant Mp*GLK* was downregulated (**Figure 4F**). We were not able to identify any strong binding motifs for GLK in either Mp*RR-MYB5* or Mp*RR-MYB2* but in the promoter of Mp*GLK* consensus binding sites for *RR-MYBs* were clearly evident (**Figure 4G**). The promoters of Mp*RR-MYB5* and Mp*GLK* each contained their own binding site indicating the potential for self-regulation.

We next tested the extent to which MpRR-MYB2, MpRR-MYB5 or MpGLK transcription factors could rescue the pale phenotype of single Mp*rr-myb5,* Mp*glk,* and double Mp*glk,rr-myb5* or Mp*rr-myb5,2* mutants (**Figure 5A-F**). Quantitative polymerase chain reactions confirmed that each transgene was over-expressed (**Figure S5**). Both Mp*RR-MYB5* and Mp*RR-MYB2* complemented Mp*rr-myb5* mutants (**Figure 5B, C and G**), further arguing for functional redundancy between MpRR-MYB5 and MpRR-MYB2. However, neither Mp*RR-MYB* rescued single Mp*glk* or double Mp*glk,rr-myb5* mutants (**Figure 5B, D, E and G**). When Mp*GLK* was expressed in the Mp*rr-myb5,2* double mutant background chlorophyll levels were increased by ~10% but the absolute levels were still 90% lower than wild type (**Figure 5F and H**). Consistent with functional redundancy between MpRR-MYB5 and MpRR-MYB2 we also found that Mp*GLK* partially complemented Mp*rr-myb5* single mutants **Figure 5C and G**) since chlorophyll accumulation was lower compared to Mp*GLK* overexpression in Mp*glk* mutants.

A conserved role for RR-MYBs in *Arabidopsis thaliana*

The RR-MYB/CCA1-like subfamily of MYB-related transcription factors[27,31,32] containing Mp*RR-MYB5* and Mp*RR-MYB2* are characterised by a conserved SHAQK(Y/F)F motif (**Figure S6A**). Based on phylogenetic analysis we identified eleven members of this group in *A. thaliana* (**Figure 6A, Figure S6B-E**) of which At*MYBS1,* At*MYBS2* and AT5G23650 were the closest homologs of Mp*RR-MYB5* and Mp*RR-MYB2* (**Figure S6B-E**). Re-analysis of publicly available data indicated that AT5G23650 is not expressed in photosynthetic tissues and so we focused analysis on At*MYBS1* and At*MYBS2*. Due to the functional redundancy evident for Mp*RR-MYB5* and Mp*RR-MYB2* above, double At*mybs1,mybs2* mutants were identified after CRISPR/Cas9-mediated gene editing (**Figure S7A and B**) and analysed in parallel with previously generated single At*mybs1* and At*mybs2* mutants. There were no detectable changes to rosette phenotype in the single mutants but double At*mybs1,mybs2* mutants were pale (**Figure 6C-F**), and this was most noticeable after bolting (**Figure 6G**). Confocal laser scanning microscopy revealed no detectable changes in chloroplast size or number in mesophyll cells of single mutants, but chloroplasts were smaller in the double At*mybs1,2* mutant (**Figure 6F**). Notably, chloroplasts of At*mybs1,2* mutants contained underdeveloped thylakoids (**Figure 6H**) similar to Mp*rr-myb5,2* mutants. In support of these findings, chlorophyll content in the single mutants was indistinguishable from wild-type, but was ~40% lower in the double

At*mybs1,mybs2* mutant (**Figure 6I)**, and quantification of chloroplast size demonstrated a 50% reduction in the double mutant (**Figure 6J**).

To gain insight into the types of photosynthesis genes regulated by At*MYBS1* and At*MYBS2* we performed RNA sequencing of the double mutant. 841 genes were down-regulated (*padj*-value ≤0.01, LFC ≥ 1-fold) and GO term analysis indicated that the two top biological terms impacted were response to light stimulus and photosynthesis (**Figure S7C and D**). Thus, consistent with lower levels of chlorophyll, loss of *MYBS1* and *MYBS2* in *A. thaliana* led to down-regulation of transcripts associated with photosynthesis. DNA motifs bound by GLK and the RR-MYBs have been determined.[25,30] Promoters of the At*MYBS1&2* transcription factors in *A. thaliana* contained motifs recognised by GLK as well as RR-MYBs (**Figure 6A**) implying regulatory interplay. Although the promoter of *GLK1* in *A. thaliana* has a motif associated with GLK binding (**Figure 7A**), in contrast with *M. polymorpha,* neither At*GLK1* or At*GLK2* contained any binding sites for MYBS1 or MYBS2 (**Figure 7A**). Promoters of the *CGA1* and *GNC* transcription factors that regulate photosynthesis gene expression in *A. thaliana*[9,33] also contained GLK but not MYBS predicted binding sites (**Figure 7A**). Analysis of *GLK*, *CGA1* and *GNC* transcript abundance in the At*mybs1,2* indicated no change in *GLK1* and *CGA1* but increases in *GLK2* and *GNC* (**Figure 7B**). This implies that cryptic or more distant MYBS1&2 binding sites exist for *GLK2* and *GNC,* or that indirect regulation links expression of these transcription factors.

Despite these changes to the upstream regulatory network compared with *M. polymoprha*, multiple lines of evidence point to a role for At*MYBS1&2* in the control of photosynthesis gene expression in *A. thaliana*. For example, 500 base pair promoters from 29% and 14% of photosynthesis associated genes contain MYBS1&2 and GLK binding sites respectively (**Figure 7C and Dataset S3**) and 12% contained both (**Figure 7C and Dataset S3**). As with *M. polymorpha*, permutation analysis indicated that substantially fewer photosynthesis genes contained neither motif (p-value=0.000) (**Figure 7D**). Rather, they contained significantly more GLK, RR-MYB and both GLK and RR-MYB binding sites (p-value=0.007, 0.000 and 0.000 respectively) than would be expected by chance (**Figure 7D**). Moreover, abundance of transcripts associated with chlorophyll biosynthesis, both photosystems and their light harvesting apparatus, as well as the Calvin Benson Bassham cycle were perturbed when At*MYBS1&2* were knocked out in *A. thaliana* (**Figure 7E and Figure S7E**).

Discussion

Chloroplasts allow photosynthesis, nitrogen and sulphur assimilation, as well as the biosynthesis of amino acids, fatty acids and carotenoids and so understanding their biogenesis has long been of interest.[34–38] Moreover, it is now widely recognised that photosynthesis has not been optimised by evolution, and so a targeted reengineering of the process could contribute to crop development.[6,7] Indeed, improvements in yield have been reported after over-expression of *SEDOHEPTULOSE BISPHOSPHATASE,*[39,40] faster relaxation of non-photochemical quenching of photosystem II[41] and rerouting of photorespiration.[42] A complementary approach to improving photosynthesis predicted to increase yield by up to 50% would be to convert C_3 crops to use the more efficient C_4 pathway.[43,44] Introducing C_4 photosynthesis in C_3 crops such as rice would require a remodelling of chloroplast biogenesis in mesophyll and bundle sheath cells.[45]

In land plants the GLK family of transcription factors are master regulators of chloroplast biogenesis, and CGA1 and GNC from the GATA family are considered ancillary players.[8,10,33] Overexpression of *GLK* in rice is sufficient to increase chloroplast occupancy of cells such as the bundle sheath, and thus to partially phenocopy traits associated with the efficient C_4 pathway.[36] However, we have an incomplete understanding of transcription factors allowing chloroplast development. For example, *GLK* and *CGA1/GNC* loss of function mutants still possess small chloroplasts[9] indicating that either these mutants are hypomorphic, or that additional unidentified actors control chloroplast biogenesis. Here we report two RR-MYB related transcription factors that act redundantly to control chlorophyll biosynthesis and photosynthesis associated gene expression in the bryophyte *M. polymorpha*. Homologs control chloroplast biogenesis in *A. thaliana* indicating functional conservation between these distantly related species. Interestingly, we were unable to identify null mutants lacking both GLK and RR-MYB in *M. polymorpha*. Indeed, although we used super-transformation of existing mutant alleles when attempting to generate triple mutants we did not observe white sectors. This apparent lethality of triple Mp*glk,rr-myb5,2* mutants mirrors loss-of-function mutations in plastidial pathways such as amino acid, vitamin, nucleotide or fatty acid biosynthesis, and those involved in chloroplast protein translation that result in an arrest of embryo development in *A. thaliana.*[46,47] This often appears to coincide with the globular-to-heart transition stage when chloroplasts start to differentiate. Mutants in genes encoding plastidial proteins required for import, modification and localisation of indispensable proteins in the chloroplast are also often associated with embryo lethality.[46,47] It is therefore possible that plants lacking both GLK and the RR-MYBs are unable to differentiate chloroplasts from proplastids.

The precise architecture of the gene regulatory network involving the *RR-MYBs* and *GLK* will need to be fully elucidated. However, consistent with the importance of negative feedback loops in plant development[48,49] RR-MYBs induce *GLK* and GLK then represses the *RR-MYBs*. Transcripts from both Mp*RR-MYBs* were more abundant in the Mp*glk* mutant, and *MpGLK* contained predicted binding sites for the MpRR-MYBs. In Mp*rr-myb2,5* mutant alleles, transcripts derived from Mp*GLK* were less abundant. Moreover, when the Mp*RR-MYB*s were overexpressed in the Mp*glk* mutant it

remained pale, arguing against RR-MYBs acting downstream of GLK. The stronger and broader down regulation of photosynthesis transcripts in the double Mp*rr-myb5,2* mutant compared with Mp*glk* could be due to the RR-MYBs acting upstream of GLK and other players. Alternatively, the larger response of photosynthesis transcripts in Mp*rr-myb5,2* mutants compared with Mp*glk* could be because the RR-MYBs have a broader set of targets. Although Mp*RR-MYB5* overexpression failed to upregulate Mp*GLK* transcripts, MYB transcription factors commonly act in multimeric complexes involving bHLH and WD40 proteins[50] or with MYCs proteins.[51] It is therefore possible that additional partners need to be over-expressed in combination with the RR-MYBs to increase expression of Mp*GLK*. It is also well documented that *GLK* is subject to multiple levels of regulation that can be overcome when non-native versions of the gene are mis-expressed.[36] Thus, it may be that the lack of response in Mp*GLK* after over-expression of Mp*RR-MYB*s is due to a similar regulatory system. When Mp*GLK* was mis-expressed in the double Mp*rr-myb5,2* mutant although chlorophyll content remained low (90% of wild type) it was significantly statistically increased. We interpret these data in two ways. Either Mp*GLK* is downstream of the Mp*RR-MYBs* and both classes of transcription factor are needed to drive full photosynthesis gene expression, or Mp*GLK* is permissive for very early stages of chloroplast biogenesis, but full assembly of the photosynthetic apparatus is strengthened by RR-MYBs because they positively regulate Mp*GLK* and they also control genes allowing carbon fixation. A permissive role for GLK in initiating chloroplast biogenesis is consistent with its ability to convert cell types accumulating a small to a large chloroplast compartment.[36] Based on the above, our current favoured hypothesis is that the RR-MYBs condition expression of *GLK* to permit early stages of chloroplast biogenesis. Although this conditioning can be partially overcome by over-expression of Mp*GLK* in the presence of RR-MYBs[15] in the absence of Mp*RR-MYBs* the impact of Mp*GLK* over-expression is limited.

As would be expected from the evolutionary distance, rewiring has taken place between these transcription factors and the structural photosynthesis genes they target in *A. thaliana* and *M. polymorpha*. In *M. polymorpha* both the RR-MYB and GLK appear to regulate themselves, and the RR-MYBs condition expression of GLK **(Figure 7E**). In *A. thaliana* this regulatory system is more complex. For example, regulation of At*GLK* by AtMYBS1&2 is less evident, but members of GATAs[9,33] also control photosynthesis gene expression. Moreover, inducible overexpression of At*MYBS1* in *A. thaliana* has been reported to increase expression of photosynthesis genes[24]. Although similar sets of genes were down-regulated in loss of function Mp*rr-myb5,2* mutants, we did not detect widespread upregulation of photosynthesis genes after over-expression of *M. polymorpha* RR-MYBs. Also consistent with rewiring between these species is the fact that compared with Mp*RR-MYB2*, the pale phenotype of Mp*RR-MYB5* indicates it plays a dominant role in chloroplast biogenesis while in *A. thaliana* neither single mutant was pale. Lastly, changes to the structure of the gene regulatory network associated with photosynthesis is also supported by the fact that promoters of Mp*RR-MYB5&2* contain their own binding sites, but Mp*GLK* does not. In contrast, in *A. thaliana* promoters of At*MYBS1* and At*MYBS2* possess *cis*-elements for both GLKs and the RR-

MYBs. The output is that the RR-MYBs operate upstream of GLK in *M. polymorpha* but not in *A. thaliana*.

The role of RR-MYBs in controlling chloroplast biogenesis is in fact supported by previous work. For example, in tomato LeMYBI has been reported to bind the promoter of the *RBCS* gene[52] . And, although no effect on chloroplast biogenesis was reported, a reduction in *RBCS* and the *chlorophyll a/b binding protein 1* (*CAB1*) genes expression has been reported in At*mybs1* mutants[53] . Along with transcription factors belonging to the GLK, B-Box and Nuclear Factor-Y families, random forest analysis of gene expression recently predicted that RR-MYBs regulate photosynthesis gene expression.[24] Moreover, RNA sequencing of an inducible At*MYBS1* over-expressor line showed upregulation of photosynthesis genes that we detected as downregulated in the At*mybs1,mybs2* mutant. Based on these findings we conclude that the RR-MYB class of transcription factors likely control photosynthesis in a wide range of land plants.

Penetrance of the RR-MYBs on photosynthesis gene expression and chloroplast biogenesis in *M. polymorpha* was striking, with Mp*RR-MYBs* activating genes allowing CO_2 fixation as well as light harvesting. Chloroplasts of Mp*myb5,2* mutants were ~30% smaller than those of Mp*glk* mutants, and double Mp*myb5,2* mutants were paler than those of Mp*glk*. This appears to be because RR-MYBs control an overlapping but broader set of photosynthesis genes than those downstream of GLK. Previous work supports the notion that these two classes of transcription factors have shared targets, as co-binding of RR-MYB and GLK to photosynthesis genes has been proposed.[54] Such cooperative binding of transcription factors is thought to allow greater variety of expression outputs.[55,56] The reach of the RR-MYBs appears extensive in that they control genes encoding enzymes of the Calvin Benson Bassham cycle and photorespiration but also assembly and repair of RuBisCO. It seems likely that the large number of genes encoding a wide range of components underpinning photosynthesis targeted by the RR-MYBs contributes to the severe perturbation to phenotype when their function is removed. And, when combined with loss of GLK, this may be why lethality ensues. Overall, the data are consistent with overlapping as well as distinct roles for these two classes of transcription factor.

In summary, from analysis of *M. polymorpha* and *A. thaliana* whose last common ancestor diverged around 400 million years ago we propose a model in which both RR-MYBs and GLKs operate as master regulators of photosynthesis gene expression (**Figure 7F**). In both species the RR-MYBs play a conserved role in controlling photosynthesis gene expression and their targets are broader than those documented for GLK. As RR-MYBs appear ubiquitous in land plants[27] it seems plausible they play a conserved role in chloroplast biogenesis. While we were unable to detect Mp*RR*-MYBs in the Zygnematophyceae algae that are sister to the land plants[57] they are in fact present in the Klebsormidiophyceae and Charophyceae[58,59] (**Figure S6B**) that represent the other two most closely related algal lineages to land plants. *GLK* homologs are present in green algae[57] and both GLK and RR-MYB motifs are present in promoter regions of these genes in *K. flaccidum*

and *C. braunii* (**Figure S7G**). These data imply that *RR-MYBs* operated alongside GLK to control chloroplast biogenesis before the colonisation of land by plants.

Materials & Methods

Plant growth and transformation

Marchantia polymorpha Cam-1 (male) and Cam-2 (female) were grown on half-strength Gamborg B5 medium plus vitamins (Duchefa Biochemie G0210, pH 5.8) and 1.2% (w/v) agar (Melford capsules, A20021) under continuous light at 22 °C with light intensity of 100 µmol $m^{-2}s^{-1}$. *Arabidopsis* thaliana C*ol-0* was except the At*mybs2* mutant that was in the *Col-3* background, and plants were grown on F2 soil (Levington, F20117800) under 16 hours light, 8 hours dark at 20 °C, 60% humidity, and 150 µmol m^{-2} s^{-1} light. *Arabidopsis* T-DNA insertion mutants At*mybs1* (SAIL_1184_D04) and At*mybs2* (SALK_150774) were obtained from NASC with T-DNA and zygosity confirmed by PCR (**Figure S7F and Table S2**). For gene editing guide RNAs were predicted using CasFinder tool (https://marchantia.info/tools/casfinder/). Several gRNAs (**Table S3**) per target were tested.[60] Single gRNAs were cloned[29] into the destination vector pMpGE013[61]. To complement Mp*rr-myb5* mutants, the Mp*RR-MYB5* promoter from[62] was used. For overexpression Mp*RR-MYB2* and Mp*RR-MYB5* coding sequences were synthesised (Integrated DNA Technologies) and cloned into the pUAP4 vector.[29] For complementation, guide RNA resistant Mp*GLK,*Mp*RR-MYB2* and Mp*RR-MYB5* coding sequences were synthesised (Integrated DNA Technologies) and cloned into the pUAP4 vector. OpenPlant parts used are listed in Star Methods.

To generate *A. thaliana* MYBS1/MYBS2 mutants two gRNAs per gene were cloned into the pEn-Chimera vector[63] using a modification of the gRNA-tRNA approach.[64] This placed guides into the pRU294 vector that has a codon optimised and intron-containing version of *Cas9* (*zCas9i*) driven by the egg-cell specific *pEC1.2* promoter.[65] *A. thaliana* was transformed by floral dipping[66] and genotyping performed as reported previously.[67] T2 plants with confirmed edits were analysed (**Figure S7A and B**). For thallus transformation 5 mL LB media were inoculated with 3-4 *Agrobacterium* colonies (*GV3101:* 50 µg/mL rifampicin, 25 µg/mL gentamicin) and the plasmid-specific selection antibiotic. The preculture was incubated at 28°C for 2 days at 110 rpm. 5 mL of 2 d *Agrobacterium* culture were centrifuged for 7 min at 2000 x *g*. The supernatant was removed and pellet re-suspended in 5 mL liquid KNOP (0.25g/L KH_2PO_4, 25g/L KCl, 25g/L $MgSO_4$ $7H_2O$, 100g/L $Ca(NO_3)_2$ $4H_2O$, 12.5mg $FeSO_4 7H_2O$, 30mM MES and pH5.5) plus 1% (w/v) sucrose and 100 µM acetosyringone. The culture was then incubated with shaking (120 rpm) at 28°C for 3-4 hours. Around 100 gemmae were transferred into a 6-well plate with 5 mL liquid KNOP medium supplemented with 1% (w/v) sucrose and 30 mM MES, pH 5.5, 80 µL of *Agrobacterium* culture and acetosyringone at final concentration of 100 µM. The tissue was co-cultivated with *Agrobacterium* for 3 days on a shaker at 110 rpm, at 22°C with ambient light. Using a sterile plastic pipette, the liquid was removed from each well and gemmae transferred onto plates with growth media containing the appropriate antibiotic (Chlorsulfuron 0.5 µM). To facilitate spreading of gemmae 1-2 mL sterile water was added to the petri dish. To genotype *M. polymorpha* 3 × 3 mm pieces of thalli from individual plants were placed in 1.5 mL tubes and crushed in 100 µL genotyping buffer (100 mM Tris-HCl, 1 M KCl, 1 M KCl, and 10 mM EDTA, pH 9.5). Tubes were then placed at 70 °C for

15-20 mins and 380 µL sterile water added to each tube. 5 µL aliquots of the extract were used as a template for polymerase chain reactions.

Chlorophyll determination, fluorescence measurements and imaging analysis

For chlorophyll measurements of *M. polymorpha* ~30-50mg of 10-14 days old gemmalings were used with five biological replicates per genotype. Tissue was blotted dry before weighing and then transferred into a 1.5mL microfuge tube containing 1 mL of dimethyl sulfoxide (DMSO) (D8418, Sigma Aldrich) and incubated in the dark at 65 °C for 45 minutes. Samples were allowed to cool to room temperature for approximately one hour. Chlorophyll content was then measured using a NanoDrop™One/One C Microvolume UV-Vis Spectrophotometer (ThermoFisher) following the manufacturer's instructions. Chlorophyll fluorescence measurements were carried out using a CF imager (Technologica Ltd, UK). *M. polymorpha* plants were placed in the dark for 20 mins and a minimum weak measuring light beam (<1 µmol m^{-2} s^{-1}) applied to evaluate dark-adapted minimum fluorescence (F_o), and a subsequent saturating pulse of 3000 µmol m^{-2} s^{-1} used to evaluate dark-adapted maximum fluorescence (F_m). A total of three plants were measured per genotype and treatment. 20 µM DCMU (#45463, Sigma Aldrich) was added to half-strength MS media, and thalli placed in DCMU for 24 h before chlorophyll fluorescence measurements were obtained.

For confocal laser scanning microscopy, five to seven gemma were placed within a medium-filled gene frame together with 30 µL water prior to being sealed with a cover slip. Plants were imaged immediately using a Leica SP8X spectral fluorescent confocal microscope with either a 10X air objective (HC PL APO 10×/0.40 CS2) or 20X air objective (HC PL APO 20×/0.75 CS2). Excitation laser wavelength and captured emitted fluorescence wavelength window were 488 nm, 498−516 nm for GFP, and 488 or 515nm, 670−700 nm for chlorophyll autofluorescence. For electron microscopy ~2 mm^2 sections of 5-6 individual 3-week-old thalli were harvested, fixed, embedded and imaged as previously described.[68] Chloroplast area was measured using ImageJ and the Macro in **Supplemental Information**.

RNA extraction and sequencing

For *M. polymorpha*, RNA was extracted from 3-4 two-week old gemmae using the RNeasy Plant kit (#74903, Qiagen) with RLT buffer supplemented with beta-mercaptoethanol, and residual genomic DNA removed using the Turbo DNA-free kit (# AM1907, Invitrogen). 500 ng of DNase-treated RNA was used as template for cDNA preparation (SuperScript™ IV First-Strand Synthesis System, #18091050, Invitrogen) according to manufacturer's instructions except that reverse transcription was 40 minutes and used oligo (dT)18 primers. qPCR was performed using the SYBR Green JumpStart *Taq* Ready Mix (#S4438, Sigma Aldrich) and a CFX384 RT System (Bio-Rad) thermal cycler. cDNA was diluted six times and oligonucleotides (**Table S3**) used at a final concentration of 0.5 µM. Reaction conditions comprised initial denaturation 94°C for 2 minutes followed by 40 cycles of 94°C for 15 seconds (denaturation) and 60°C for 1 minute (annealing,

extension, and fluorescence reading). Primer sequences are in **Table S3**. Library preparation and RNA sequencing was performed by Novogene (Cambridge, UK). Briefly, messenger RNA was purified from total RNA using poly-T oligo-attached magnetic beads. After fragmentation, first strand cDNA was synthesised using random hexamer primers. Library concentration was measured on a Qubit instrument using the manufacturer's procedure (Thermo Fisher Scientific) followed by real-time qPCR quantification. Library size distribution was analysed on a bioanalyzer (Agilent) following the manufacturer's protocol. Quantified libraries were pooled and sequenced on a NovaSeq PE150 Illumina platform and 6G raw data per sample obtained. Adapter sequences were: 5' Adapter: 5'-AGATCGGAAGAGCGTCGTGTAGGGAAAGAGTGTAGATCTCGGTGGTCGCCGTATCATT-3'. 3' Adapter: 5'-GATCGGAAGAGCACACGTCTGAACTCCAGTCACGGATGACTATCTCGTATGCCGTCTTCTGCTTG-3'

FastQC was used to assess read quality and TrimGalore (https://doi.org/10.5281/zenodo.5127899) to remove low-quality reads and adapters. Reads were pseudo-aligned using Kallisto[69] to the *M. polymorpha* genome version 5 (primary transcripts only, obtained from MarpolBase)[70]. Mapping statistics for each library are provided in **Supplemental Dataset 2**. DGE analysis was performed with DESeq2 [71], with padj-values < 0.01.

Phylogenetic analysis

To identify RR Myb-related/CCA1-like genes three approaches were combined. Firstly, RR Myb-related/CCA1-like genes for twenty-one plant genomes were mined from iTAK[72] and PlantTFDB[73], Phytozome, Fernbase[74], Phycozome and PhytoPlaza databases. Sequences for each species were aligned with the MpRR-MYB5 and *A. thaliana* MYBS1 and MYBS2 amino acid sequences using MAFFT[75]. Results were filtered manually to identify RR-Myb-related/CCA1-like orthologs distinguished from other Myb-related genes based on the conserved SHAKYF motif in the R1/2 domain. Secondly, BLASTP searches were performed against plant genomes in Phytozome v13, fern genomes (fernbase.org), hornworts genome (www.hornworts.uzh.ch)[76], green algae genomes in PhycoCosm (/phycocosm.jgi.doe.gov), and 1KP using the MpRR-MYB5 and *A. thaliana* MYBS1 and MYBS2 amino acid amino acid sequence. Identified RR-Myb-related/CCA1-like protein sequences were aligned using MAFFT and trimmed using TrimAl[77]. A maximum likelihood phylogenetic tree was inferred using iQTree[78], ModelFinder[79] and ultrafast approximation for phylogenetic bootstrap[80] and SH-aLRT test[81]. The tree was visualised using iTOL.[82] Full list of sequences in **Dataset S4**.

RR-MYB and GLK binding site analysis

AtGLK1 and GLK2 transcription factor binding motifs were taken from ChIP-seq data.[25] AtMYBS1 and MYBS2 binding sites (motifs MA1186.1 and MA1399.1) were obtained from JASPAR.[83] GLK

and MYBS motifs were merged to create GLK combined and RR-MYB combined motifs and visualised using the Ceqlogo tool from MEME.[84] The FIMO tool[85] was used to scan promoter sequences of *A. thaliana* and *M. polymorpha* for matches to transcription factor binding motifs found in the JASPAR motif database.[83] To account for input sequence composition, a background model was generated using the fasta-get-markov tool from the MEME suite.[84] FIMO was then run with default parameters and a P value cut-off of 1×10^{-4}. Matches to GLK and RR-MYB combined motifs were highlighted in each output. To assess occurrence of GLK and RR-MYB motifs in photosynthesis gene promoter sequences (500 bp upstream of the TSS) were scanned using FIMO[85]. Promoters were then scored for presence or absence of each motif and percentage of photosynthesis of genes containing each calculated. To test the background distribution of RR-MYB and GLK motifs a set of random promoters of the same size as the list of photosynthesis genes from *M. polymorpha* or *A. thaliana* was extracted and FIMO ran to determine the presence of these motifs. This process was iterated 1000 times and distributions of the frequency of these motifs plotted. The frequency of motifs in promoters of photosynthesis genes was also determined by searching each promoter with FIMO. Permutation tests were performed to test whether the frequency of motifs was significantly different to the frequency found in random selected promoters **(File S1).**

Author contributions

N.Y.E., E.F. and J.M.H. designed the work. N.Y.E., E.F., K.B., T.S., M.T. and P.D. carried out the work. N.Y.E, E.F. and J.M.H. wrote the manuscript with input from all authors.

Acknowledgements

This work was funded as part of the BBSRC/EPSRC OpenPlant Synthetic Biology Research Centre Grant BB/ L014130/1 to J.P.H., BBSRC BB/F011458/1 for confocal microscopy to J.P.H and BBSRC sLOLA BBP0031171 and ERACAPS grant C4BREED to J.M.H. T.B.S. was supported by a SNSF Postdoc Mobility Fellowship (P500PB_203128) and EMBO Long-Term Fellowship (ALTF 531-2019). For the purpose of open access, the authors have applied a Creative Commons Attribution (CC BY) licence to any Author Accepted Manuscript version arising from this submission. We thank Karin H. Müller, Filomena Gallo and Georgina E. Lindop from the Cambridge Advanced Imaging Centre for the electron microscopy sample preparation as well as the support during the image acquisition. We also thank Facundo Romani for useful comments and support during the project.

REFERENCES

1. Archibald, J.M. (2009). The Puzzle of Plastid Evolution. Current Biology *19*, 81–88.

2. McFadden, G.I. (2014). Origin and Evolution of Plastids and Photosynthesis in Eukaryotes. Cold Spring Harb. Perspect. Biol. *6*, a016105.

3. Gould, S.B., Waller, R.F., and McFadden, G.I. (2008). Plastid Evolution. Annual Review of Plant Biology *59*, 491–517.

4. Abdallah, F., Salamini, F., and Leister, D. (2000). A prediction of the size and evolutionary origin of the proteome of chloroplasts of Arabidopsis. Trends Plant Sci. *5*, 141–142.

5. Martin, W., Rujan, T., Richly, E., Hansen, A., Cornelsen, S., Lins, T., Leister, D., Stoebe, B., Hasegawa, M., and Penny, D. (2002). Evolutionary analysis of Arabidopsis, cyanobacterial, and chloroplast genomes reveals plastid phylogeny and thousands of cyanobacterial genes in the nucleus. Proc. Natl. Acad. Sci. U. S. A. *99*, 12246–12251.

6. Long, S.P., Marshall-Colon, A., and Zhu, X.-G. (2015). Meeting the global food demand of the future by engineering crop photosynthesis and yield potential. Cell *161*, 56–66.

7. Ort, D.R., Merchant, S.S., Alric, J., Barkan, A., Blankenship, R.E., Bock, R., Croce, R., Hanson, M.R., Hibberd, J.M., Long, S.P., et al. (2015). Redesigning photosynthesis to sustainably meet global food and bioenergy demand. Proc. Natl. Acad. Sci. U. S. A. *112*, 8529–8536.

8. Cackett, L., Luginbuehl, L.H., Schreier, T.B., Lopez-Juez, E., and Hibberd, J.M. (2022). Chloroplast development in green plant tissues: the interplay between light, hormone, and transcriptional regulation. New Phytol. *233*, 2000–2016.

9. Zubo, Y.O., Blakley, I.C., Franco-Zorrilla, J.M., Yamburenko, M.V., Solano, R., Kieber, J.J., Loraine, A.E., and Schaller, G.E. (2018). Coordination of Chloroplast Development through the Action of the GNC and GLK Transcription Factor Families. Plant Physiol. *178*, 130–147.

10. Waters, M.T., Wang, P., Korkaric, M., Capper, R.G., Saunders, N.J., and Langdale, J.A. (2009). GLK transcription factors coordinate expression of the photosynthetic apparatus in Arabidopsis. Plant Cell *21*, 1109–1128.

11. Naito, T., Kiba, T., Koizumi, N., Yamashino, T., and Mizuno, T. (2007). Characterization of a unique GATA family gene that responds to both light and cytokinin in Arabidopsis thaliana. Biosci. Biotechnol. Biochem. *71*, 1557–1560.

12. Fitter, D.W., Martin, D.J., Copley, M.J., Scotland, R.W., and Langdale, J.A. (2002). *GLK*gene pairs regulate chloroplast development in diverse plant species. The Plant Journal *31*, 713–727.

13. Wang, P., Fouracre, J., Kelly, S., Karki, S., Gowik, U., Aubry, S., Shaw, M.K., Westhoff, P., Slamet-Loedin, I.H., Paul Quick, W., et al. (2013). Evolution of GOLDEN2-LIKE gene function in C3 and C4 plants. Planta *237*, 481.

14. Yasumura, Y., Moylan, E.C., and Langdale, J.A. (2005). A conserved transcription factor mediates nuclear control of organelle biogenesis in anciently diverged land plants. Plant Cell *17*, 1894–1907.

15. Yelina, N.E., Frangedakis, E., Schreier, T.B., Rever, J., Tomaselli, M., Haseloff, J., and Hibberd, J.M. (2023). Streamlined regulation of chloroplast development in the liverwort Marchantia polymorpha. bioRxiv, 2023.01.23.525199. 10.1101/2023.01.23.525199.

16. Chiang, Y.-H., Zubo, Y.O., Tapken, W., Kim, H.J., Lavanway, A.M., Howard, L., Pilon, M., Kieber, J.J., and Schaller, G.E. (2012). Functional characterization of the GATA transcription factors GNC and CGA1 reveals their key role in chloroplast development, growth, and division in Arabidopsis. Plant Physiol. *160*, 332–348.

17. Bowman, J.L., Arteaga-Vazquez, M., Berger, F., Briginshaw, L.N., Carella, P., Aguilar-Cruz, A., Davies, K.M., Dierschke, T., Dolan, L., Dorantes-Acosta, A.E., et al. (2022). The renaissance and enlightenment of Marchantia as a model system. Plant Cell *34*, 3512–3542.

18. Schwechheimer, C., Schröder, P.M., and Blaby-Haas, C.E. (2022). Plant GATA Factors: Their Biology, Phylogeny, and Phylogenomics. Annu. Rev. Plant Biol. *73*, 123–148.

19. Flores-Sandoval, E., Romani, F., and Bowman, J.L. (2018). Co-expression and Transcriptome Analysis of Transcription Factors Supports Class C ARFs as Independent Actors of an Ancient Auxin Regulatory Module. Front. Plant Sci. *9*, 1345.

20. Sullivan, A.M., Arsovski, A.A., Lempe, J., Bubb, K.L., Weirauch, M.T., Sabo, P.J., Sandstrom, R., Thurman, R.E., Neph, S., Reynolds, A.P., et al. (2014). Mapping and Dynamics of Regulatory DNA and Transcription Factor Networks in A. thaliana. Cell Reports *8*, 2015–2030.

21. Bastakis, E. (2017). The Contribution of the GATA Transcription Factors GNC and GNL in the Greening of Arabidopsis Thaliana. *The Plant Cell*, *30*(3), 582–599.

22. Bursch, K., Toledo-Ortiz, G., Pireyre, M., Lohr, M., Braatz, C., and Johansson, H. (2020). Identification of BBX proteins as rate-limiting cofactors of HY5. Nat Plants *6*, 921–928.

623 23. Zhao, P., Cui, R., Xu, P., Wu, J., Mao, J.-L., Chen, Y., Zhou, C.-Z., Yu, L.-H., and Xiang, C.-B.
624 (2017). ATHB17 enhances stress tolerance by coordinating photosynthesis associated
625 nuclear gene and ATSIG5 expression in response to abiotic stress. Sci. Rep. *7*, 45492.

626 24. Halpape, W., Wulf, D., Verwaaijen, B., Stasche, A.S., Zenker, S., Sielemann, J., Tschikin, S.,
627 Viehöver, P., Sommer, M., Weber, A.P.M., et al. (2023). Transcription factors mediating
628 regulation of photosynthesis. bioRxiv, 2023.01.06.522973. 10.1101/2023.01.06.522973.

629 25. Tu, X., Ren, S., Shen, W., Li, J., Li, Y., Li, C., Li, Y., Zong, Z., Xie, W., Grierson, D., et al.
630 (2022). Limited conservation in cross-species comparison of GLK transcription factor binding
631 suggested wide-spread cistrome divergence. Nat. Commun. *13*, 7632.

632 26. Dubos, C., Stracke, R., Grotewold, E., Weisshaar, B., Martin, C., and Lepiniec, L. (2010). MYB
633 transcription factors in Arabidopsis. Trends in Plant Science *15*, 573–581.

634 27. Du, H., Wang, Y.-B., Xie, Y., Liang, Z., Jiang, S.-J., Zhang, S.-S., Huang, Y.-B., and Tang, Y.-
635 X. (2013). Genome-wide identification and evolutionary and expression analyses of MYB-
636 related genes in land plants. DNA Res. *20*, 437–448.

637 28. Trebst, A. (2007). Inhibitors in the functional dissection of the photosynthetic electron transport
638 system. Photosynth. Res. *92*, 217–224.

639 29. Sauret-Güeto, S., Frangedakis, E., Silvestri, L., Rebmann, M., Tomaselli, M., Markel, K.,
640 Delmans, M., West, A., Patron, N.J., and Haseloff, J. (2020). Systematic Tools for
641 Reprogramming Plant Gene Expression in a Simple Model,. ACS Synth. Biol. *9*, 864–882.

642 30. O'Malley, R.C., Huang, S.-S.C., Song, L., Lewsey, M.G., Bartlett, A., Nery, J.R., Galli, M.,
643 Gallavotti, A., and Ecker, J.R. (2016). Cistrome and Epicistrome Features Shape the
644 Regulatory DNA Landscape. Cell *166*, 1598.

645 31. Pu, X., Yang, L., Liu, L., Dong, X., Chen, S., Chen, Z., Liu, G., Jia, Y., Yuan, W., and Liu, L.
646 (2020). Genome-Wide Analysis of the MYB Transcription Factor Superfamily in Physcomitrella
647 patens. International Journal of Molecular Sciences *21*, 975.

648 32. Yanhui, C., Xiaoyuan, Y., Kun, H., Meihua, L., Jigang, L., Zhaofeng, G., Zhiqiang, L., Yunfei,
649 Z., Xiaoxiao, W., Xiaoming, Q., et al. (2006). The MYB transcription factor superfamily of
650 Arabidopsis: expression analysis and phylogenetic comparison with the rice MYB family. Plant
651 Mol. Biol. *60*, 107–124.

652 33. Bastakis, E., Hedtke, B., Klermund, C., Grimm, B., and Schwechheimer, C. (2018). LLM-
653 Domain B-GATA Transcription Factors Play Multifaceted Roles in Controlling Greening in
654 Arabidopsis. Plant Cell *30*, 582–599.

655 34. Witte, C.-P., and Herde, M. (2020). Nucleotide Metabolism in Plants. Plant Physiol. *182*, 63–
656 78.

657 35. Waters, M.T., and Langdale, J.A. (2009). The making of a chloroplast. EMBO J. *28*, 2861–
658 2873.

659 36. Wang, P., Khoshravesh, R., Karki, S., Tapia, R., Balahadia, C.P., Bandyopadhyay, A., Quick,
660 W.P., Furbank, R., Sage, T.L., and Langdale, J.A. (2017). Re-creation of a Key Step in the
661 Evolutionary Switch from C3 to C4 Leaf Anatomy. Curr. Biol. *27*, 3278–3287.

662 37. Jarvis, P., and López-Juez, E. (2013). Biogenesis and homeostasis of chloroplasts and other
663 plastids. Nat. Rev. Mol. Cell Biol. *14*, 787–802.

664 38. López-Juez, E. (2007). Plastid biogenesis, between light and shadows. J. Exp. Bot. *58*, 11–26.

665 39. Lefebvre, S., Lawson, T., Zakhleniuk, O.V., Lloyd, J.C., Raines, C.A., and Fryer, M. (2005).
666 Increased sedoheptulose-1,7-bisphosphatase activity in transgenic tobacco plants stimulates
667 photosynthesis and growth from an early stage in development. Plant Physiol. *138*, 451–460.

668 40. Driever, S.M., Simkin, A.J., Alotaibi, S., Fisk, S.J., Madgwick, P.J., Sparks, C.A., Jones, H.D.,
669 Lawson, T., Parry, M.A.J., and Raines, C.A. (2017). Increased SBPase activity improves
670 photosynthesis and grain yield in wheat grown in greenhouse conditions. Philos. Trans. R.
671 Soc. Lond. B Biol. Sci. *372*.

672 41. Kromdijk, J., Głowacka, K., Leonelli, L., Gabilly, S.T., Iwai, M., Niyogi, K.K., and Long, S.P.
673 (2016). Improving photosynthesis and crop productivity by accelerating recovery from
674 photoprotection. Science *354*, 857–861.

675 42. South, P.F., Cavanagh, A.P., Liu, H.W., and Ort, D.R. (2019). Synthetic glycolate metabolism
676 pathways stimulate crop growth and productivity in the field. Science *363*, eaat9077.

677 43. Hibberd, J.M., Sheehy, J.E., and Langdale, J.A. (2008). Using C4 photosynthesis to increase
678 the yield of rice-rationale and feasibility. Curr. Opin. Plant Biol. *11*, 228–231.

679 44. von Caemmerer, S., Quick, W.P., and Furbank, R.T. (2012). The development of C_4rice:
680 current progress and future challenges. Science *336*, 1671–1672.

681 45. Langdale, J.A. (2011). C4 cycles: past, present, and future research on C4 photosynthesis.
682 Plant Cell *23*, 3879–3892.

683 46. Budziszewski, G.J., Lewis, S.P., Glover, L.W., Reineke, J., Jones, G., Ziemnik, L.S.,
684 Lonowski, J., Nyfeler, B., Aux, G., Zhou, Q., et al. (2001). Arabidopsis genes essential for

seedling viability: isolation of insertional mutants and molecular cloning. Genetics *159*, 1765–1778.

47. Bryant, N., Lloyd, J., Sweeney, C., Myouga, F., and Meinke, D. (2011). Identification of nuclear genes encoding chloroplast-localized proteins required for embryo development in Arabidopsis. Plant Physiol. *155*, 1678–1689.

48. Somssich, M., Je, B.I., Simon, R., and Jackson, D. (2016). CLAVATA-WUSCHEL signaling in the shoot meristem. Development *143*, 3238–3248.

49. Jamsheer K, M., Jindal, S., Sharma, M., Awasthi, P., S, S., Sharma, M., Mannully, C.T., and Laxmi, A. (2022). A negative feedback loop of TOR signaling balances growth and stress-response trade-offs in plants. Cell Rep. *39*, 110631.

50. Ramsay, N.A., and Glover, B.J. (2005). MYB-bHLH-WD40 protein complex and the evolution of cellular diversity. Trends Plant Sci. *10*, 63–70.

51. Dickinson, P.J., Kneřová, J., Szecówka, M., Stevenson, S.R., Burgess, S.J., Mulvey, H., Bågman, A.-M., Gaudinier, A., Brady, S.M., and Hibberd, J.M. (2020). A bipartite transcription factor module controlling expression in the bundle sheath of Arabidopsis thaliana. Nat Plants *6*, 1468–1479.

52. Rose, A., Meier, I., and Wienand, U. (1999). The tomato I-box binding factor LeMYBI is a member of a novel class of myb-like proteins. Plant J. *20*, 641–652.

53. Chen, Y.-S., Chao, Y.-C., Tseng, T.-W., Huang, C.-K., Lo, P.-C., and Lu, C.-A. (2017). Two MYB-related transcription factors play opposite roles in sugar signaling in Arabidopsis. Plant Mol. Biol. *93*, 299–311.

54. Tu, X., Mejía-Guerra, M.K., Valdes Franco, J.A., Tzeng, D., Chu, P.-Y., Shen, W., Wei, Y., Dai, X., Li, P., Buckler, E.S., et al. (2020). Reconstructing the maize leaf regulatory network using ChIP-seq data of 104 transcription factors. Nat. Commun. *11*, 5089.

55. Ibarra, I.L., Hollmann, N.M., Klaus, B., Augsten, S., Velten, B., Hennig, J., and Zaugg, J.B. (2020). Mechanistic insights into transcription factor cooperativity and its impact on protein-phenotype interactions. Nat. Commun. *11*, 124.

56. Sönmezer, C., Kleinendorst, R., Imanci, D., Barzaghi, G., Villacorta, L., Schübeler, D., Benes, V., Molina, N., and Krebs, A.R. (2021). Molecular Co-occupancy Identifies Transcription Factor Binding Cooperativity In Vivo. Mol. Cell *81*, 255–267.

57. Cheng, S., Xian, W., Fu, Y., Marin, B., Keller, J., Wu, T., Sun, W., Li, X., Xu, Y., Zhang, Y., et al. (2019). Genomes of Subaerial Zygnematophyceae Provide Insights into Land Plant Evolution. Cell *179*, 1057–1067.

58. Hori, K., Maruyama, F., Fujisawa, T., Togashi, T., Yamamoto, N., Seo, M., Sato, S., Yamada, T., Mori, H., Tajima, N., et al. (2014). Klebsormidium flaccidum genome reveals primary factors for plant terrestrial adaptation. Nat. Commun. *5*, 3978.

59. Nishiyama, T., Sakayama, H., de Vries, J., Buschmann, H., Saint-Marcoux, D., Ullrich, K.K., Haas, F.B., Vanderstraeten, L., Becker, D., Lang, D., et al. (2018). The Chara Genome: Secondary Complexity and Implications for Plant Terrestrialization. Cell *174*, 448–464.

60. Yelina, N.E., Holland, D., Gonzalez-Jorge, S., Hirsz, D., Yang, Z., and Henderson, I.R. (2022). Coexpression of MEIOTIC-TOPOISOMERASE VIB-dCas9 with guide RNAs specific to a recombination hotspot is insufficient to increase crossover frequency in Arabidopsis. G3 *12*.

61. Sugano, S.S., Nishihama, R., Shirakawa, M., Takagi, J., Matsuda, Y., Ishida, S., Shimada, T., Hara-Nishimura, I., Osakabe, K., and Kohchi, T. (2018). Efficient CRISPR/Cas9-based genome editing and its application to conditional genetic analysis in Marchantia polymorpha. PLoS One *13*, e0205117.

62. Romani, F., Sauret-Güeto, S., Rebmann, M., Annese, D., Bonter, I., Tomaselli, M., Dierschke, T., Delmans, M., Frangedakis, E., Silvestri, L., et al. (2023). Mapping the landscape of transcription factor promoter activity during vegetative development in Marchantia. bioRxiv, 2023.06.17.545419. 10.1101/2023.06.17.545419.

63. Fauser, F., Schiml, S., and Puchta, H. (2014). Both CRISPR/Cas-based nucleases and nickases can be used efficiently for genome engineering in Arabidopsis thaliana. Plant J. *79*, 348–359.

64. Xie, K., Minkenberg, B., and Yang, Y. (2015). Boosting CRISPR/Cas9 multiplex editing capability with the endogenous tRNA-processing system. Proc. Natl. Acad. Sci. U. S. A. *112*, 3570–3575.

65. Ursache, R., Fujita, S., Dénervaud Tendon, V., and Geldner, N. (2021). Combined fluorescent seed selection and multiplex CRISPR/Cas9 assembly for fast generation of multiple Arabidopsis mutants. Plant Methods *17*, 111.

66. Logemann, E., Birkenbihl, R.P., Ülker, B., and Somssich, I.E. (2006). An improved method for preparing Agrobacterium cells that simplifies the Arabidopsis transformation protocol. Plant Methods *2*, 16.

67. Edwards, K., Johnstone, C., and Thompson, C. (1991). A simple and rapid method for the preparation of plant genomic DNA for PCR analysis. Nucleic Acids Res. *19*, 1349.

68. Schreier, T.B., Müller, K.H., Eicke, S., Faulkner, C., Zeeman, S.C., and Hibberd, J.M. (2023). Plasmodesmal connectivity in C Gynandropsis gynandra is induced by light and dependent on photosynthesis. New Phytol. 10.1111/nph.19343.

69. Bray, N.L., Pimentel, H., Melsted, P., and Pachter, L. (2016). Near-optimal probabilistic RNA-seq quantification. Nat. Biotechnol. *34*, 525–527.

70. Bowman, J.L., Kohchi, T., Yamato, K.T., Jenkins, J., Shu, S., Ishizaki, K., Yamaoka, S., Nishihama, R., Nakamura, Y., Berger, F., et al. (2017). Insights into Land Plant Evolution Garnered from the Marchantia polymorpha Genome. Cell *171*, 287–304.e15.

71. Love, M.I., Huber, W., and Anders, S. (2014). Moderated estimation of fold change and dispersion for RNA-seq data with DESeq2. Genome Biol. *15*, 550.

72. Zheng, Y., Jiao, C., Sun, H., Rosli, H.G., Pombo, M.A., Zhang, P., Banf, M., Dai, X., Martin, G.B., Giovannoni, J.J., et al. (2016). iTAK: A Program for Genome-wide Prediction and Classification of Plant Transcription Factors, Transcriptional Regulators, and Protein Kinases. Mol. Plant *9*, 1667–1670.

73. Jin, J., Tian, F., Yang, D.-C., Meng, Y.-Q., Kong, L., Luo, J., and Gao, G. (2017). PlantTFDB 4.0: toward a central hub for transcription factors and regulatory interactions in plants. Nucleic Acids Res. *45*, 1040–1045.

74. Li, F.-W., Brouwer, P., Carretero-Paulet, L., Cheng, S., de Vries, J., Delaux, P.-M., Eily, A., Koppers, N., Kuo, L.-Y., Li, Z., et al. (2018). Fern genomes elucidate land plant evolution and cyanobacterial symbioses. Nat Plants *4*, 460–472.

75. Katoh, K., and Standley, D.M. (2013). MAFFT multiple sequence alignment software version 7: improvements in performance and usability. Mol. Biol. Evol. *30*, 772–780.

76. Li, F.-W., Nishiyama, T., Waller, M., Frangedakis, E., Keller, J., Li, Z., Fernandez-Pozo, N., Barker, M.S., Bennett, T., Blázquez, M.A., et al. (2020). Anthoceros genomes illuminate the origin of land plants and the unique biology of hornworts. Nat Plants *6*, 259–272.

77. Capella-Gutiérrez, S., Silla-Martínez, J.M., and Gabaldón, T. (2009). trimAl: a tool for automated alignment trimming in large-scale phylogenetic analyses. Bioinformatics *25*, 1972–1973.

78. Nguyen, L.-T., Schmidt, H.A., von Haeseler, A., and Minh, B.Q. (2015). IQ-TREE: a fast and effective stochastic algorithm for estimating maximum-likelihood phylogenies. Mol. Biol. Evol. *32*, 268–274.

79. Kalyaanamoorthy, S., Minh, B.Q., Wong, T.K.F., von Haeseler, A., and Jermiin, L.S. (2017). ModelFinder: fast model selection for accurate phylogenetic estimates. Nature Methods *14*, 587–589. 10.1038/nmeth.4285.

80. Hoang, N.V., Pfeifer, L., Feringa, B.L., and Pshenichnikov, M.S. (2020). Ultrafast Dynamics of Molecular Motors Driven by Near-Infrared Light. The 22nd International Conference on Ultrafast Phenomena 2020. 10.1364/up.2020.th3a.1.

81. Guindon, S., Dufayard, J.-F., Lefort, V., Anisimova, M., Hordijk, W., and Gascuel, O. (2010). New algorithms and methods to estimate maximum-likelihood phylogenies: assessing the performance of PhyML 3.0. Syst. Biol. *59*, 307–321.

82. Letunic, I., and Bork, P. (2019). Interactive Tree Of Life (iTOL) v4: recent updates and new developments. Nucleic Acids Res. *47*, 256–259.

83. Fornes, O., Castro-Mondragon, J.A., Khan, A., van der Lee, R., Zhang, X., Richmond, P.A., Modi, B.P., Correard, S., Gheorghe, M., Baranašić, D., et al. (2020). JASPAR 2020: update of the open-access database of transcription factor binding profiles. Nucleic Acids Res. *48*, 87–92.

84. Bailey, T.L., Boden, M., Buske, F.A., Frith, M., Grant, C.E., Clementi, L., Ren, J., Li, W.W., and Noble, W.S. (2009). MEME SUITE: tools for motif discovery and searching. Nucleic Acids Res. *37*, 202–208.

85. Grant, C.E., Bailey, T.L., and Noble, W.S. (2011). FIMO: scanning for occurrences of a given motif. Bioinformatics *27*, 1017–1018.

800 **FIGURE**

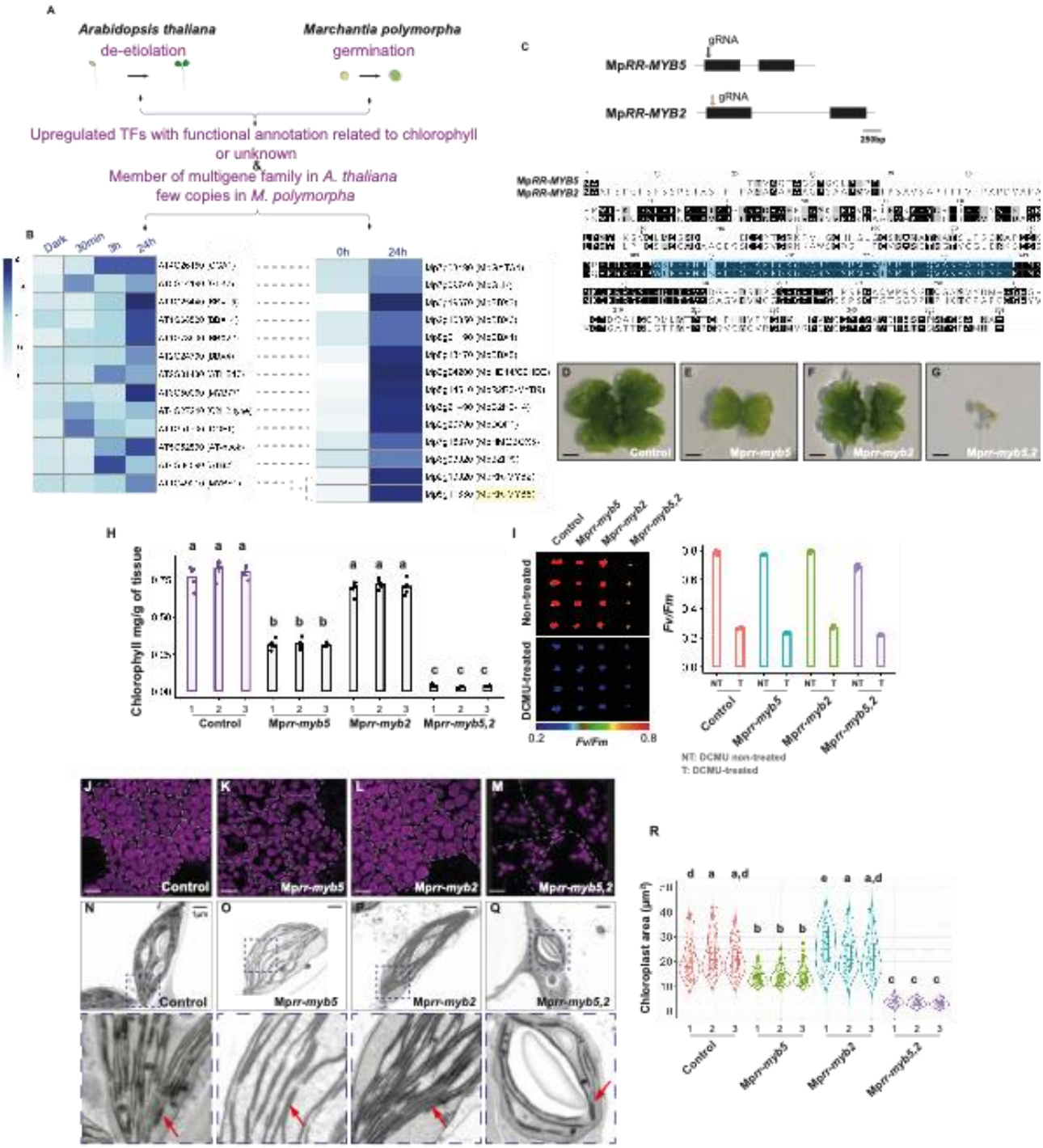

801

Figure 1: Mp*RR-MYB5* and Mp*RR-MYB2* act redundantly to regulate chloroplast biogenesis in *M. polymorpha*. A) Schematic of pipeline used to identify candidate transcription factors regulating photosynthesis gene expression. RNA sequencing data from *Arabidopsis thaliana* during de-etiolation[19] and *Marchantia polymorpha* during spore germination[20] were examined. Transcription factors (TFs) upregulated in response to light in both species with either unknown or related to chlorophyll function were retained. As we hypothesised that functional redundancy had hindered identification of such regulators via forward genetic screens an additional criterion was that each family should be represented by multiple copies in *A. thaliana* but by a maximum of two in *M. polymorpha*. **B)** Heatmaps showing transcript abundance (z-score) of candidates that were selected to generate knockout mutants in *M. polymorp*ha. **C)** Left: Schematic of Mp*RR-MYB5* and Mp*RR-MYB2* gene structure (exons represented as black boxes) with guide (g) RNAs for CRISPR represented by arrows. Right: Amino acid sequence alignments of MpRR-MYB5 and MpRR-MYB2 proteins with the characteristic RR-MYB/CCA1-like domain is highlighted in blue. **D-G)** Representative images of control and Mp*rr-myb5,* Mp*rr-myb2* and Mp*rr-myb5,2* mutants. Scale bars represent 2 mm. **H)** Chlorophyll content of Mp*rr-myb5*, Mp*rr-myb2* and Mp*rr-myb5,2* mutants. Letters show statistical ranking using a *post hoc* Tukey test with different letters indicating statistically significant differences at $p<0.01$. Values indicated by the same letter are not statistically different. n=5. **I)** Representative images and quantification after imaging of the chlorophyll fluorescence parameter F_v/F_m with and without the inhibitor Di-Chlorophenyl Di-methyl Urea (DCMU). Although the Mp*rr-myb5,* Mp*rr-myb2* and Mp*rr-myb5,2* mutants have lower chlorophyll content, the drop in F_v/F_m values after treatment with DCMU indicates that photosystem II is functional. **J-M)** Representative images after confocal laser scanning microscopy of Mp*rr-myb5*, Mp*rr-myb2* and Mp*rr-myb5,2* mutants with chlorophyll autofluorescence shown in magenta. Cell borders are marked with dashed white lines. Scale bars represent 10 µm. **N-Q)** Representative images after transmission electron microscopy of Mp*rr-myb5*, Mp*rr-myb2* and Mp*rr-myb5,2* mutants. Scale bars represent 1 µm. The dashed area depicted in each chloroplast is enlarged and grana stacks indicated with red arrows. **R)** Violin plots of chloroplast area for the Mp*rr-myb5,* Mp*rr-myb2* and Mp*rr-myb5,2* mutants. Box and whiskers represent the 25 to 75 percentile and minimum-maximum distributions of the data. Letters show statistical ranking using a *post hoc* Tukey test with different letters indicating statistically significant differences at $p<0.01$. Values indicated by the same letter are not statistically different, n=150.

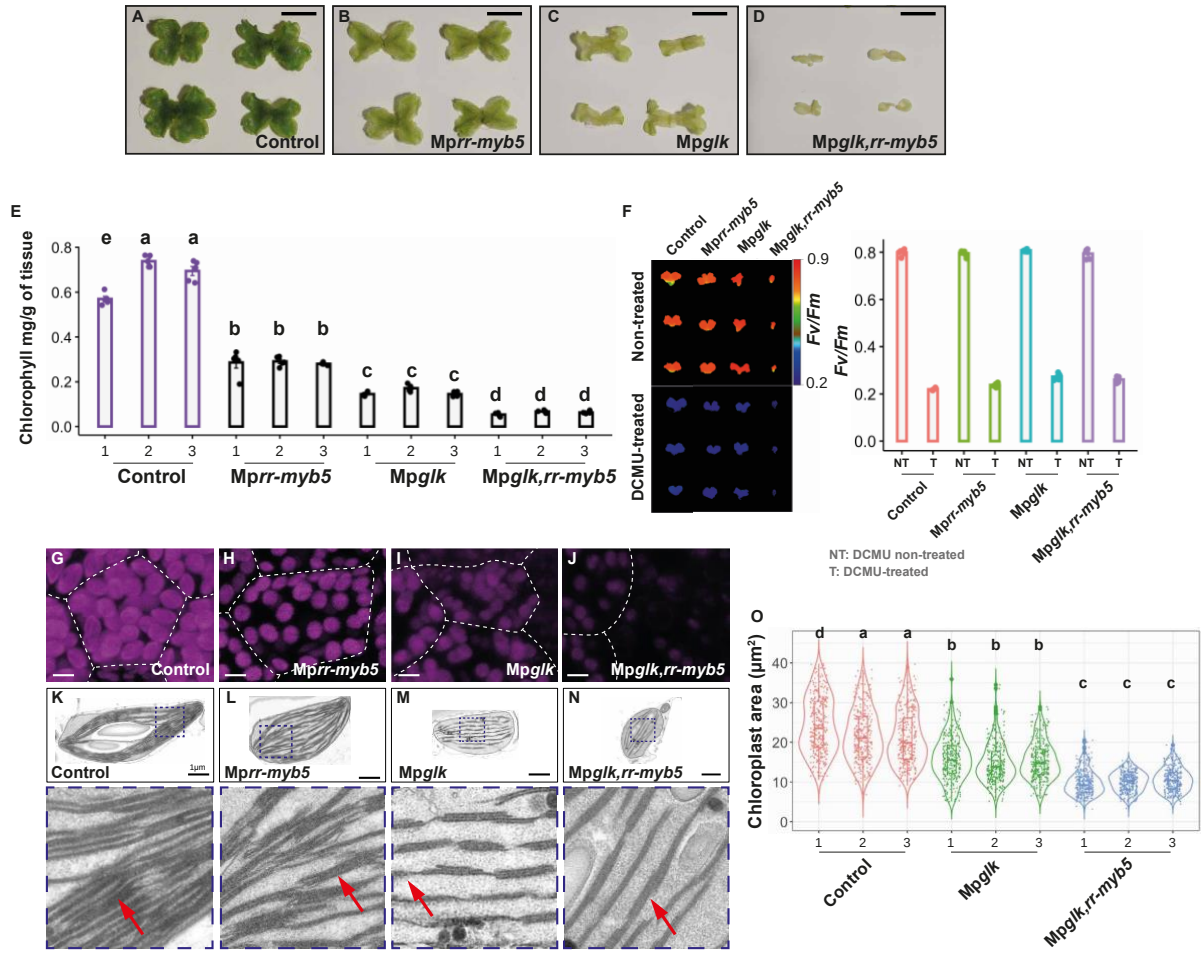

Figure 2: MpRR-MYB5 acts synergistically with MpGLK to control chloroplast biogenesis. A-D) Representative images of control, Mp*glk*, Mp*rr-myb5* and Mp*glk,rr-myb5* mutants. Scale bars represent 7 mm. **E)** Chlorophyll content is lower in Mp*glk*, Mp*rr-myb5* and the double Mp*glk,rr-myb5* mutants compared with controls. Letters show statistical ranking using a *post hoc* Tukey test with different letters indicating statistically significant differences at $p<0.01$. Values indicated by the same letter are not statistically different, n=5. **F)** Representative images and quantification after imaging of the chlorophyll fluorescence parameter F_v/F_m with and without the inhibitor Di-Chlorophenyl Di-methyl Urea (DCMU). Mp*rr-myb5,* Mp*glk* and Mp*glk,rr-myb5* mutants have lower chlorophyll content, the drop in F_v/F_m values after treatment with DCMU indicates that photosystem II is functional. **G-J)** Representative images after confocal laser scanning microscopy of control, Mp*rr-myb5,* Mp*glk* and Mp*glk,rr-myb5* mutants. Chlorophyll autofluorescence shown in magenta, cell borders marked with dashed white lines. Scale bars represent 10 µm. **K-N)** Representative images from transmission electron microscopy images of control, Mp*rr-myb5,* Mp*glk* and Mp*glk,rr-myb5* mutants. Scale bars represent 1 µm. The dashed area depicted in each chloroplast is enlarged and granal stacks indicated with red arrows. **O)** Chloroplast area of Mp*glk* and Mp*glk,rr-myb5* mutants. Box and whiskers represent the 25 to 75 percentile and minimum-maximum distributions of the data. Letters show statistical ranking using a *post hoc* Tukey test with different letters indicating statistically significant differences at $p<0.01$. Values indicated by the same letter are not statistically different. n=330.

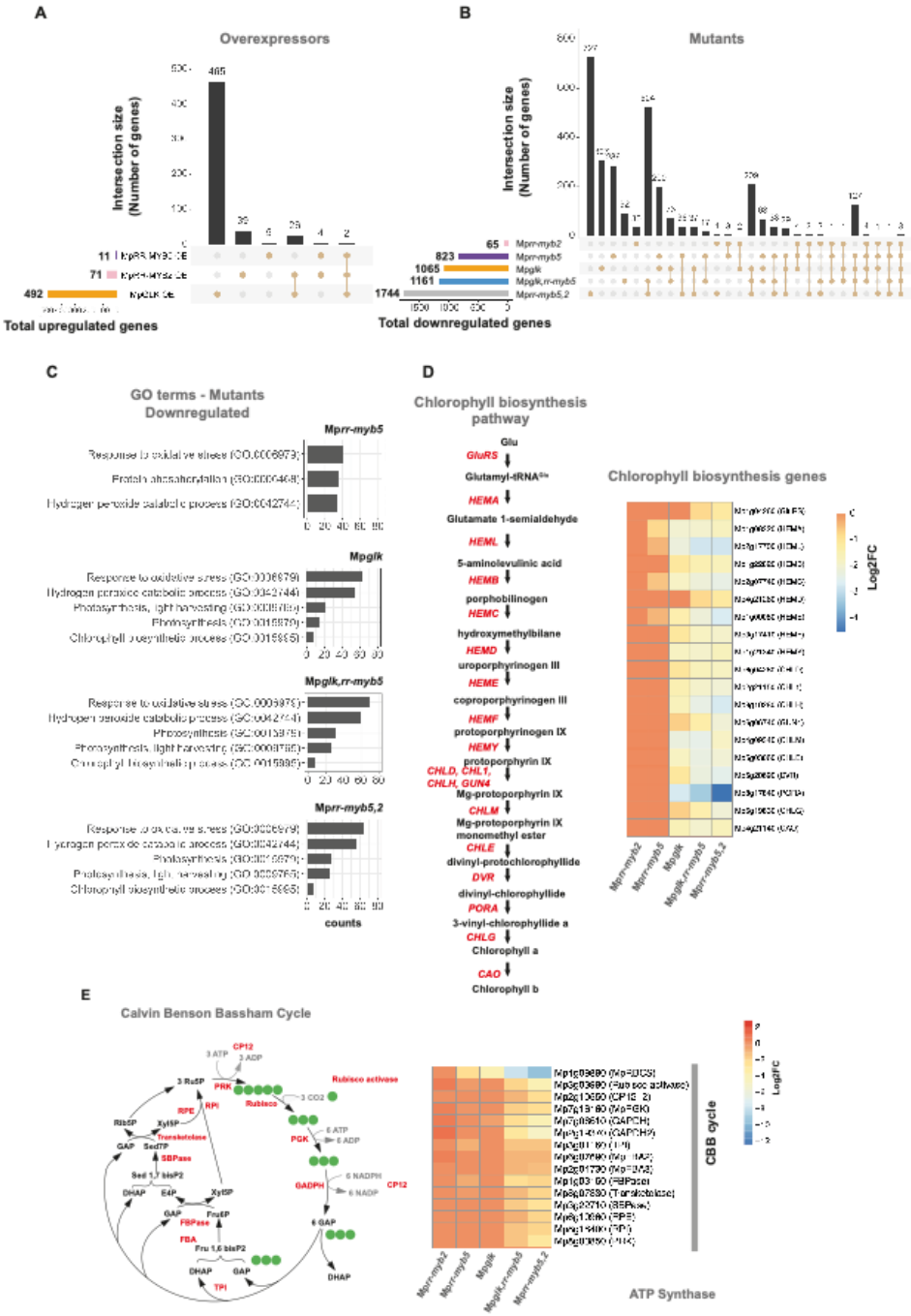

Figure 3: Mp*RR-MYB5* and Mp*RR-MYB2* regulate expression of genes encoding chlorophyll biosynthesis and the Calvin Benson Bassham cycle. A) Upset diagram showing sets of upregulated genes in Mp*RR-MYB5,* Mp*RR-MYB2* and Mp*GLK* over-expression lines. **B)** Upset diagram showing sets of downregulated genes in Mp*glk*, Mp*rr-myb2,* Mp*rr-myb5,* and the double Mp*glk,rr-myb5* or Mp*rr-myb5,2* mutants. **C)** Enriched Gene Ontology terms for Mp*rr-myb5,* Mp*glk,rr-myb5,* Mp*glk* and Mp*rr-myb5,2* mutants. **D)** Heatmap illustrating the extent of down-regulation of transcripts encoding enzymes of chlorophyll biosynthesis in Mp*rr-myb2,* Mp*rr-myb5, Mpglk,* and the *Mpglk,rr-myb5* or Mp*rr-myb5,2* mutant alleles. **E)** Heatmap indicating lower transcript abundance of genes encoding components of Calvin-Benson-Bassham cycle in Mp*glk*, Mp*rr-myb5,* Mp*rr-myb2* as well as Mp*glk,rr-myb5*,*myb2* and Mp*rr-myb5*,*myb2* double mutants. Modified from Lea and Leegood, 1998.

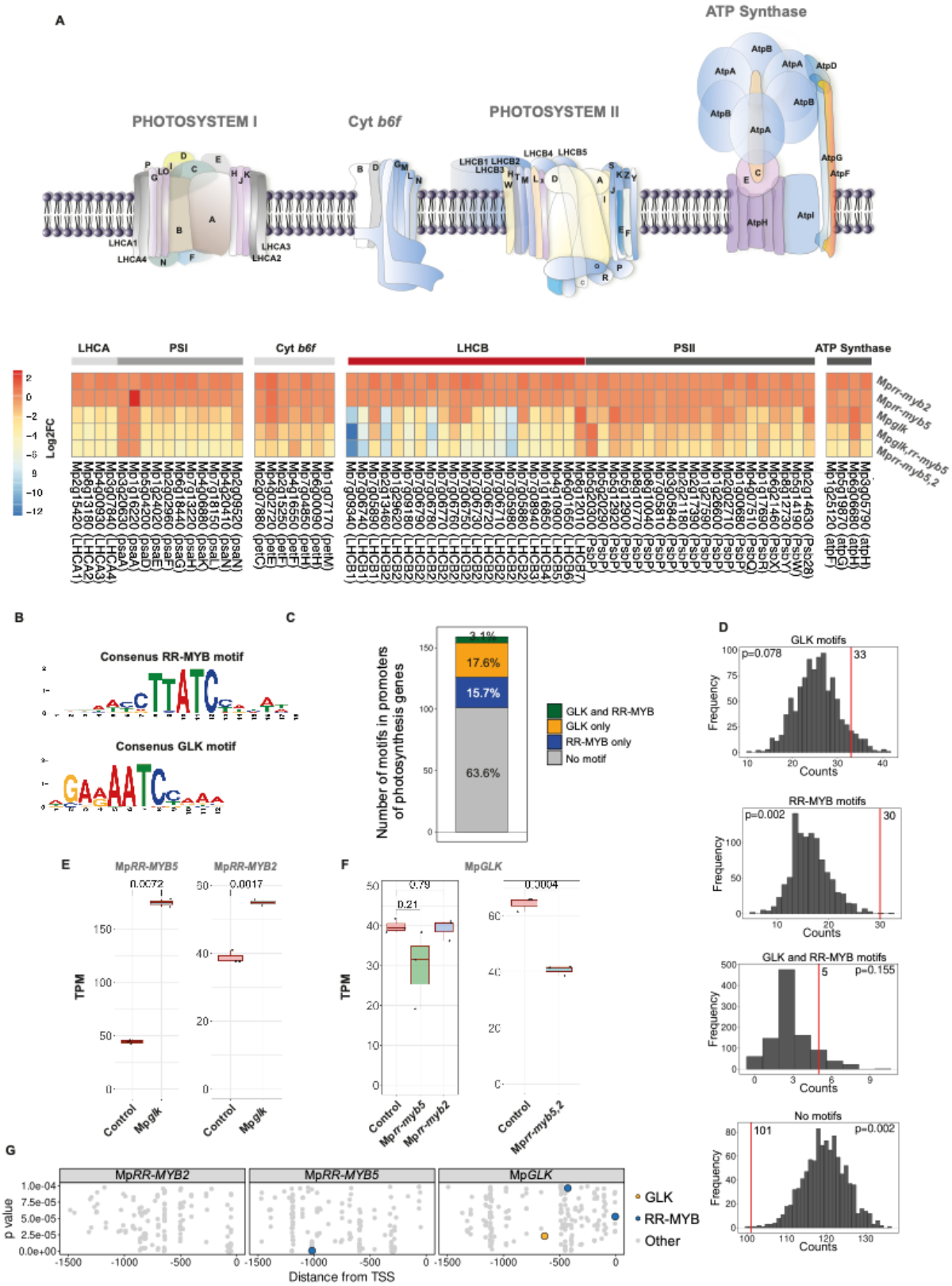

Figure 4: Combined loss of Mp*RR-MYB5&2* has greater impact on abundance of transcripts encoding the light harvesting apparatus than loss of Mp*GLK* and down-regulates GLK expression. A) Heatmap indicating lower transcript abundance of genes encoding components of Photosystem II, Photosystem I and the cytochrome b_6f complex in Mp*glk*, Mp*rr-myb5,* Mp*rr-myb2* as well as Mp*glk,rr-myb5*,*myb2* and Mp*rr-myb5*,*myb2* double mutants. The greatest degree of down regulation was detected in the double Mp*rr-myb5,2* double mutant. Schematic modified from[10] and [25]. **B)** Consensus motif sequence logo for RR-MYB and GLK transcription factors. **C)** Bar chart showing RR-MYB and GLK binding sites within 500bp upstream of the predicted transcriptional start site (TSS) in *M. polymorpha* photosynthesis genes. **D)** Histograms showing the distribution of motifs in 500bp promoters of 1000 random gene sets. Red line indicates the frequency of the motif in *M. polymorpha* photosynthesis genes. P-values calculated by permutation testing. **E-F)** Transcripts abundance of Mp*GLK,* Mp*RR-MYB2* and Mp*RR-MYB5* in control, Mp*rr-glk,* Mp*rr-myb5,* Mp*rr-myb2* and Mp*rr-myb5*,*2* mutant backgrounds. Data presented as Transcript Per Million (TPM), and P-values of two-tailed *t*-test are shown. **G)** Scatter plots showing position and predicted binding affinity of GLK, RR-MYB binding and other motifs upstream of Mp*GLK,* Mp*RR-MYB2* and Mp*RR-MYB5* TSS, the y-axis shows p-values of matches between upstream regions and motif position weight matrices, and x-axis shows position of the motif center relative to the TSS. P-values calculated by log-likelihood score using FIMO.

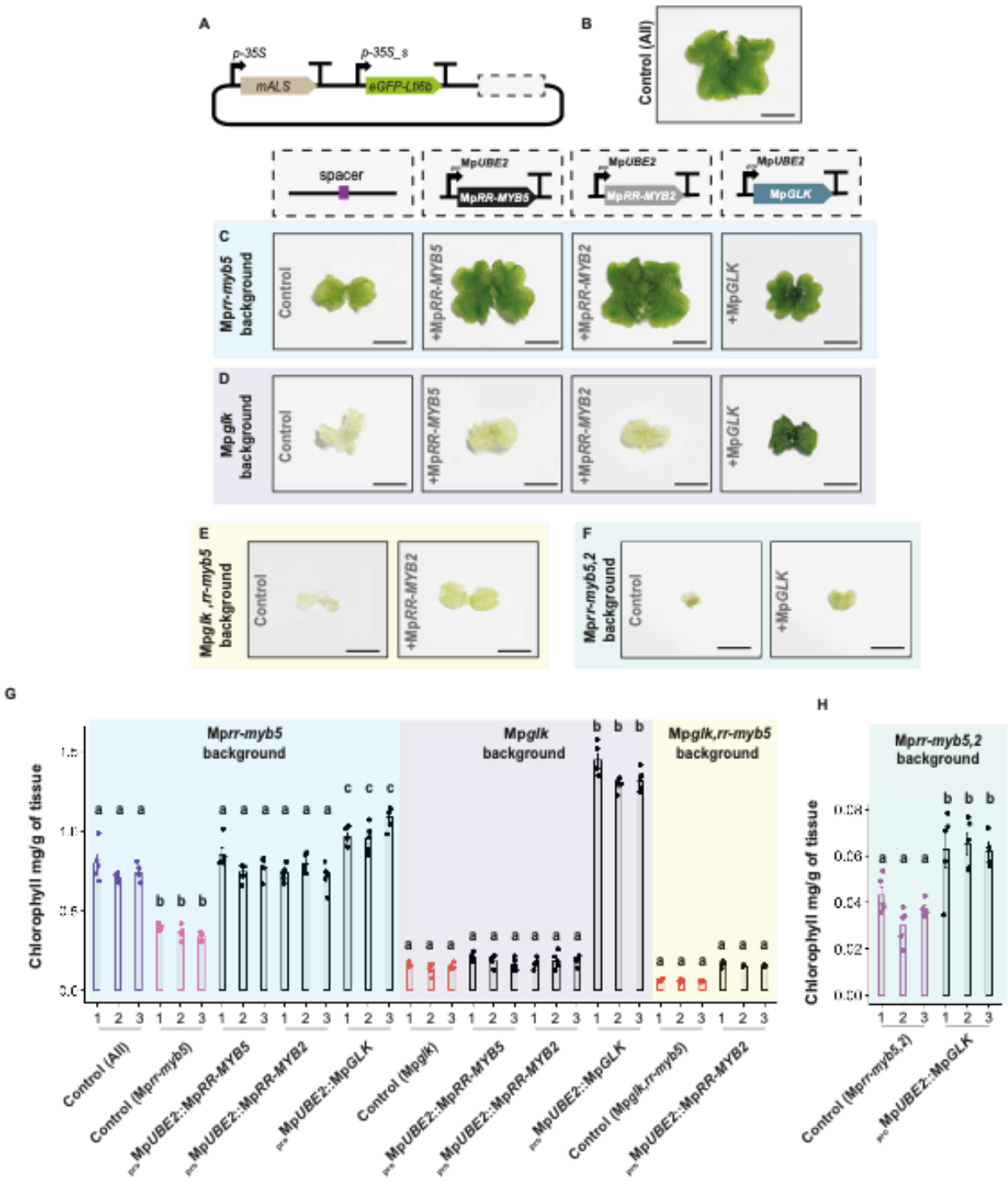

Figure 5: *M. polymorpha* RR-MYBs do not complement Mp*GLK*: A) Schematic representation of constructs used to overexpress Mp*RR-MYB5,* Mp*RR-MYB2* and Mp*GLK.* **B)** Representative image of control plants. Scale bar represents 5 mm. **C-F)** Representative images of Mp*rr-myb5,* Mp*glk,* Mp*glk,rr-myb5* and Mp*rr-myb5,2* mutants complemented with Mp*RR-MYB5,* Mp*RR-MYB2* and Mp*GLK.* Scale bars represent 2mm. **G-H)** Chlorophyll content in control, Mp*rr-myb5,* Mp*glk,* Mp*glk,rr-myb5* and Mp*rr-myb5,2* mutants complemented with Mp*RR-MYB5,* Mp*RR-MYB2* and Mp*GLK.* Letters show statistical ranking using a *post hoc* Tukey test (comparisons are made between groups highlighted with the same colour rectangle, different letters indicating statistically significant differences at P<0.01). Values indicated by the same letter are not statistically different n=5.

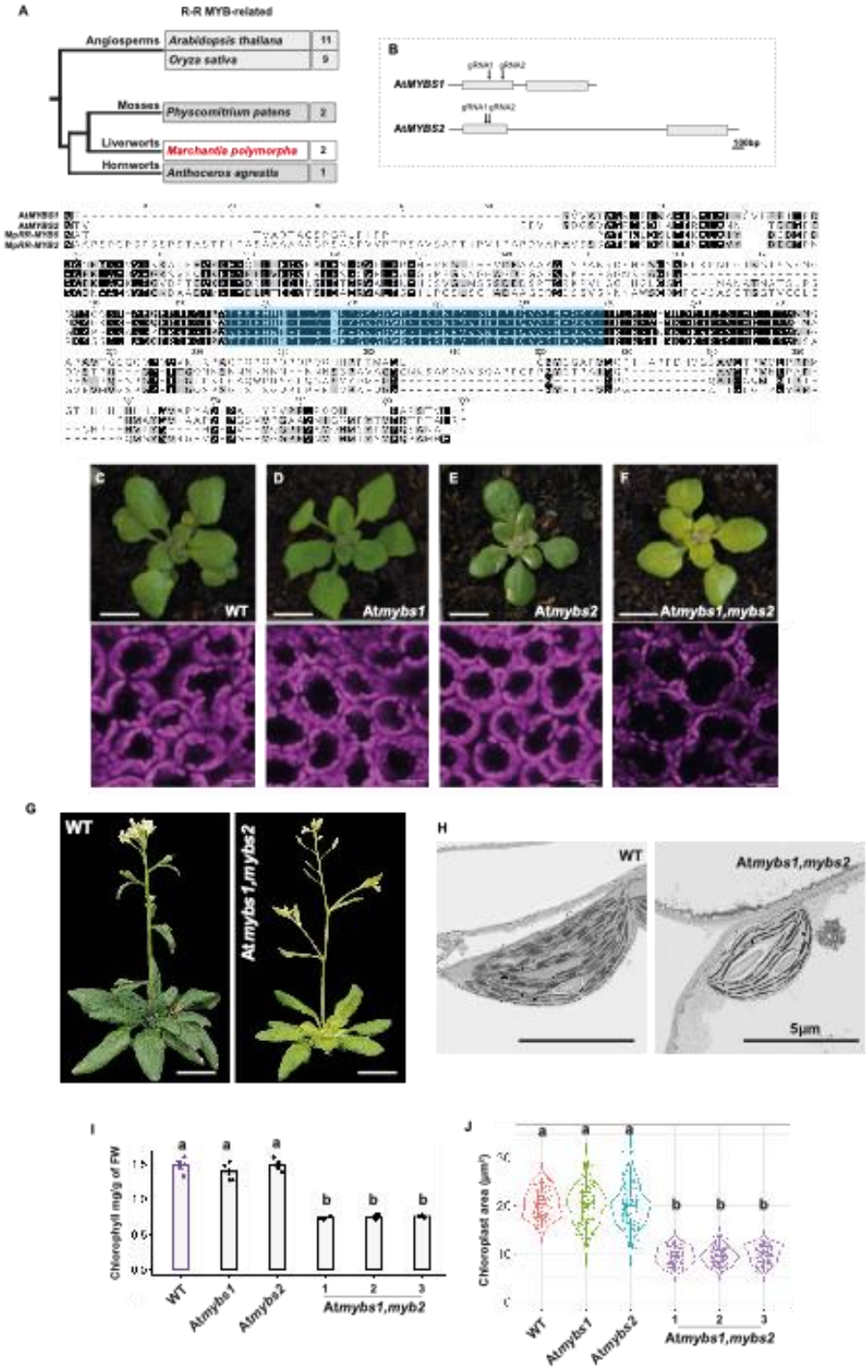

974
975

Figure 6: RR-MYBs control chlorophyll biogenesis in *A. thaliana.* A) Number of RR-Myb-Related transcription factors in *A. thaliana*, rice and bryophytes. Amino acid alignment of the two MpRR-MYB factors in *M. polymorpha* (red arrowheads) and *A. thaliana* MYBS1 and MYBS2 (bottom). Characteristic gene domains are shown as coloured boxes. **B)** Schematic representation of At*MYBS1* and At*MYBS2* gene structure showing exons as grey rectangles. guide (g) RNAs positions for gene editing shown with arrows. **C-F)** Images of two-week old seedlings of wild type, At*mybs1,* At*mybs2* and At*mybs1,mybs2* mutants (scale bars represent 7 mm. Representative images after confocal laser scanning microscopy also shown (bottom) with scale bars representing 25 µm. **G)** Images of wild type and At*mybs1,mybs2* mutants with inflorescence. Scale bars represent 1.5 cm. **H)** Representative transmission electron microscopy images of wild type and At*mybs1,mybs2* mutants. Scale bars represent 5 µm. **I)** Bar plots of chlorophyll content for wild type, At*mybs1,* At*mybs2* and At*mybs1,mybs2* mutants (three independent lines were used for measurements). Letters show statistical ranking using a *post hoc* Tukey test (with different letters indicating statistically significant differences at $P<0.01$). Values indicated by the same letter are not statistically different, n=5. **J)** Violin plots of chloroplast area for wild type, At*mybs1,* At*mybs2* and At*mybs1,mybs2* mutants. Box and whiskers represent the 25 to 75 percentile and minimum-maximum distributions of the data. Letters show statistical ranking using a *post hoc* Tukey test (with different letters indicating statistically significant differences at $P<0.01$). Values indicated by the same letter are not statistically different. n=100.

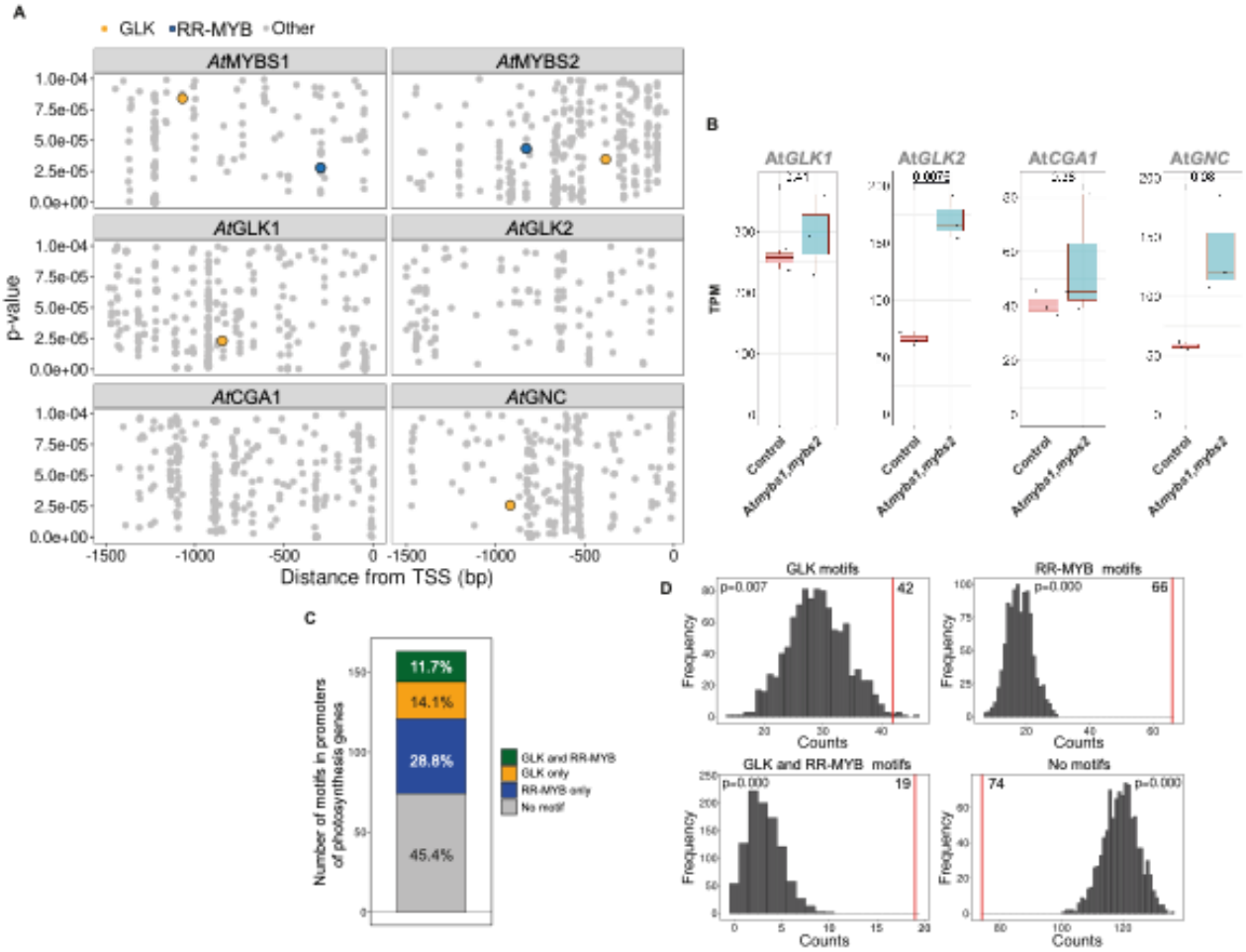

E

Chlorophyll biosynthesis

Gene	log2FC
AT3G48730 (GSA1)	-0.973404
AT5G08280 (HEMC)	-0.997152
AT2G40490 (HEME2)	-1.842105
AT5G18660 (DVR)	-0.908167
AT1G03630 (PORC)	-0.941689

Calvin Benson Bassham Cycle

Gene	log2FC
AT5G38410 (RBCS3B)	-1.158661
AT5G38420 (RBCS2B)	-1.34528
AT3G12780 (PGK1)	-1.033306
AT1G12900 (GAPA2)	-0.942342
AT1G55490 (CPNB1)	-0.8513
AT2G28000 (CPNA1)	-0.919179

Photorespiration

Gene	log2FC
AT2G35370 (GDHC)	-1.432987
AT1G32470 (GDC-H1)	-1.568028
AT1G32080 (Lrg8)	-0.953238

Light harvesting

Gene	log2FC	
AT3G54890 (LHCA1)	-1.23513	LHCA
AT3G61470 (LHCA2)	-1.315061	LHCA
AT1G61520 (LHCA3)	-1.175695	LHCA
AT3G47470 (LHCA4)	-1.169918	LHCA
AT4G02770 (PsaD1)	-1.122695	PSI
AT4G28750 (PsaE1)	-1.125835	PSI
AT2G20260 (PsaE2)	-1.456162	PSI
AT1G31330 (PsaF)	-1.073336	PSI
AT1G55670 (PsaG)	-0.895592	PSI
AT3G16140 (PsaH1)	-1.077185	PSI
AT1G52230 (PsaH2)	-1.438544	PSI
AT1G08380 (PsaO)	-0.867905	PSI
AT1G30380 (PsaK)	-0.957567	PSI
AT2G46820 (PsaP)	-1.1607	PSI

Gene	log2FC	
AT1G29920 (LHCB1.1)	-1.10071	LHCB
AT1G29910 (LHCB1.2)	-0.904924	LHCB
AT1G29930 (LHCB1.3)	-1.761318	LHCB
AT2G34430 (LHCB1.4)	-6.082789	LHCB
AT2G34420 (LHCB1.5)	-1.049355	LHCB
AT5G54270 (LHCB3)	-1.386108	LHCB
AT5G01530 (LHCB4.1)	-1.3085	LHCB
AT3G08940 (LHCB4.2)	-0.929136	LHCB
AT4G10340 (LHCB5)	-0.811321	LHCB
AT1G15820 (LHCB6)	-1.561819	LHCB
AT5G66570 (PsbQ1)	-0.817722	PSII
AT4G05180 (PsbQ2)	-1.016175	PSII
AT2G30570 (PsbW)	-1.180948	PSII
AT2G06520 (PsbX)	-0.955055	PSII
AT3G21055 (PsbT)	-1.588563	PSII
AT4G21280 (PsbQ1)	-0.988605	PSII
AT1G51400 (Psb5)	-1.755429	PSII

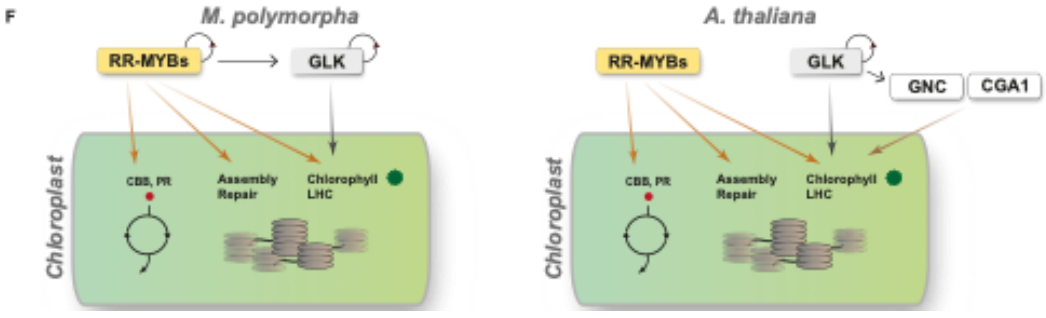

1008

Figure 7: Loss of At*MYBS1&2* downregulates expression of genes encoding chlorophyll biosynthesis enzymes, the Calvin Benson Bassham cycle as well as those encoding the light harvesting apparatus. **A)** Scatter plots showing position and predicted binding affinity of GLK, RR-MYB binding and other motifs upstream of At*GLK1,* At*GLK2,* At*MYBS1* and At*MYBS2* transcriptional start site (TSS). Y-axis shows p-values of matches between upstream regions and motif position weight matrices, and x-axis shows position of the motif center relative to the TSS. P-values calculated by log-likelihood score using FIMO. **B)** Transcript abundance in Transcripts Per Million (TPM) of At*GLK1,* At*GLK2,* At*CGA1* and At*GNC* in wild-type and At*mybs1,mybs2* mutant background. P-values of two-tailed *t*-test are shown. **C)** Barchart showing GLK and RR-MYB binding sites within 500bp upstream of the transcriptional start site (TSS) in *A. thaliana* photosynthesis genes **D)** Histograms showing the distribution of motifs in 500bp promoters of 1000 random gene sets. Red line indicates the frequency of the motif in *A.thaliana* photosynthesis genes. P-values calculated by permutation testing. **E)** List of Chlorophyll biosynthesis, Calvin Benson Bassham (CBB) cycle, Photorespiration and Light harvesting genes downregulated in At*mybs1,mybs2* mutants. **F)** Model illustrating role of RR-MYBs in the control of chloroplast biogenesis. In the bryophyte *M. polymorpha* (left), RR-MYBs act upstream of GLK. Both MpRR-MYB and MpGLK appear to regulate themselves through feedforward loops. Whilst MpGLK regulates photosynthesis genes associated with chlorophyll biosynthesis and sub-units of the light harvesting complexes (LHC), RR-MYBs also regulate genes of the Calvin Benson Bassham (CBB) cycle and photorespiration (PR) as well as assembly and repair of the photosystems. In the angiosperm model *A. thaliana* (right) RR-MYBs no longer act upstream of *GLK* but they do regulate genes of the Calvin Benson Bassham (CBB) cycle and photorespiration (PR) as well as assembly and repair of the photosystems. At*GLK* regulates itself but also At*GNC*, and as with *M. polymorpha*, it controls photosynthesis genes associated with chlorophyll biosynthesis and sub-units of the light harvesting complexes (LHC).